Possible effects of shorter-chained poly-and perfluoroalkyl substances (PFAS) exposure on metabolic processes

Nilesh Arulchelvam

Thesis submitted to the University of Ottawa in partial fulfillment of the requirements for the MSc degree in Biochemistry

Department of Biochemistry, Microbiology and Immunology
Faculty of Medicine
University of Ottawa

ABSTRACT

The extensive use of per- and polyfluoroalkyl substances (PFAS) have sparked significant public health concerns due to their increased persistence in the environment and negative impacts on human health. Developing evidence has suggested perfluorooctanoic acid (PFOA), a well known PFAS, to contribute to the formation of metabolic syndrome. The replacement of PFOA with shorter-chained perfluoroalkyl carboxylic acids (PFCAs), such as perfluoroheptanoic acid (PFHpA) and perfluorohexanoic acid (PFHxA), has been rising. However, their impact on adipogenesis and the development of metabolic syndrome is unknown. The aim of this study was to investigate the effect of PFOA, PFHpA and PFHxA on adipogenesis in 3T3-L1 preadipocytes. All three chemicals induced adipogenesis at higher concentrations. Results demonstrated increased adipogenic marker expression and increased lipid accumulation within cells, upon PFCA treatment. We then looked at the activation of PPARγ and PPARα upon PFCA treatments. Results showed that PFOA activated both PPARγ and PPARα, while PFHpA and PFHxA only activated PPARα, suggesting that the mechanism which PFHpA and PFHxA induce adipogenesis is PPARα-mediated. Further research is required to confirm the mechanism which PFOA induces adipogenesis.

RÉSUMÉ

L'utilisation intensive de substances per- et polyfluoroalkyles (PFAS) a suscité d'importantes préoccupations de santé publique en raison de leur persistance accrue dans l'environnement et de leurs impacts négatifs sur la santé humaine. De plus en plus de preuves suggèrent que l'acide perfluorooctanoïque (PFOA), un PFAS bien connu, contribue à la formation du syndrome métabolique. Le remplacement du PFOA par des acides perfluoroalkylcarboxyliques (PFCA) à chaîne plus courte, tels que l'acide perfluoroheptanoïque (PFHpA) et l'acide perfluorohexanoïque (PFHxA), est en augmentation. Cependant, leur impact sur l'adipogenèse et le développement du syndrome métabolique est inconnu. Le but de cette étude était d'étudier l'effet du PFOA, du PFHpA et du PFHxA sur l'adipogenèse dans les préadipocytes 3T3-L1. Les trois produits chimiques ont induit l'adipogenèse à des concentrations plus élevées. Les résultats ont démontré une expression accrue des marqueurs adipogènes et une accumulation accrue de lipides lors du traitement par PFCA. Nous avons ensuite examiné l'activation de PPARγ et PPARα lors de traitements par PFCA. Les résultats ont montré que le PFOA activait à la fois PPARγ et PPARα, tandis que PFHpA et PFHxA n'activaient que PPARα, ce qui suggère que le mécanisme par lequel PFHpA et PFHxA induisent l'adipogenèse est médié par PPARα. Des recherches supplémentaires sont nécessaires pour confirmer le mécanisme par lequel le PFOA induit l'adipogenèse.

ACKNOWLEDGEMENTS

I would like to extend my gratitude to my supervisor, Dr. Ella Atlas, for her guidance and support throughout the challenges and triumphs of my research journey. Her expertise has been very helpful, enabling me to navigate the complexities of my project.

Additionally, I would like to thank Dr. Céline Aguer and Dr. Erin Mulvihill, dedicated members of my Thesis Advisory Committee, whose insightful advice and ideas have consistently sparked new directions in my research. Their contributions have been instrumental in broadening my perspective and enhancing the quality of my work. I am truly grateful for their unwavering support throughout my time as a Master's student. Their guidance and encouragement have been instrumental in my academic journey.

Lastly, I am eternally thankful for the unwavering love and support of my family and friends. Their encouragement to pursue my Master's degree, even in the face of challenges, has been a cornerstone of my perseverance. Their belief in my abilities has provided me with such motivation and strength, without which this journey would have been immeasurably more difficult.

TABLE OF CONTENTS

LIST OF ABBREVIATIONS

Acacb: Acetyl-Coenzyme A carboxylase beta

ACOX1: acyl-CoA oxidase 1

Adig: Adipogenin

Adipoq: Adiponectin

AFFF: Aqueous film-foaming foam

Agt: Angiotensinogen

AKT: Protein kinase B

aP2: Adipocyte protein 2

ATP: Adenosine triphosphate

BCS: Bovine calf serum

cAMP: Cyclic adenosine monophosphate

Ccnd1: Cyclin D1

Cdkn1a: Cyclin-dependent kinase inhibitor 1A

C/EBPα: CCAAT/enhancer binding protein α

C/EBPβ: CCAAT/enhancer binding protein β

C/EBPδ: CCAAT/enhancer binding protein δ

C-F: Carbon-fluorine

Cfd: adipsin

CPT1b: Carnitine palmitoyltransferase 1B

CRE: cAMP response element

CREB: cAMP response element-binding protein

CRM: Cell recovery media

CSM: Compound screening media

CVD: Cardiovascular diseases

Dlk1: Delta-like 1 homolog (Drosophila)

DMSO: Dimethylsulfoxide

DMEM: Dulbecco’s modified Eagle’s medium

E2f1: E2F transcription factor 1

EDC: Endocrine disrupting chemicals

EDTA: Ethylenediamine tetraacetic acid

Egr2: Early growth response 2

FBS: Fetal bovine serum

FABP4: Fatty acid binding protein 4

Fasn: Fatty acid synthase

Fgf2: Fibroblast growth factor 2

Foxc2: Forkhead box C2

Foxo1: Forkhead box O1

Gata2: GATA binding protein 2

Gata3: GATA binding protein 3

GLUT4: Glucose transporter type 4

GPCR: G protein-coupled receptors

GR: Glucocorticoid receptors

IBMX: 1-methyl-3-isobutyl-xanthine

IR: Insulin receptor

IRS1: Insulin receptor substrate-1

IRS2: Insulin receptor substrate-2

K_d: Sediment-water partition coefficient

Klf15: Kruppel-like factor 15

Klf2: Kruppel-like factor 2 (lung)

LDR: Luciferase detection reagent

Lep: Leptin

Lipe : Lipase

LPL: Lipoprotein lipase

MCE: Mitotic clonal expansion

NAFLD: Non-alcoholic fatty liver disease

Ncor2: Nuclear receptor co-repressor 2

Nr0b2: Nuclear receptor subfamily 0, group B, member 2

Nrlh3: Liver X receptor alpha

OECD: Organization for Economic Cooperation and Development

PBS: Phosphate-buffered saline

PDK1: 3-phosphoinositide-dependent protein kinases-1

PFAS: Per- and polyfluoroalkyl substances

PFCA: Perfluoroalkyl carboxylic acid

PFHxA: Perfluorohexanoic acid

PFHpA: Perfluoroheptanoic acid

PFOA: Perfluorooctanoic acid

PFOS: Perfluorooctanesulfonic acid

PFSA: Perfluoroalkane sulfonic acids

PI3-K: Phosphoinositide 3-kinase

PKA: Protein kinase A

PPAR: Peroxisome proliferator-activated receptor

PPARα: Peroxisome proliferator-activated receptor α

PPARβ: Peroxisome proliferator-activated receptor β

PPARδ: Peroxisome proliferator-activated receptor δ

PPARγ: Peroxisome proliferator-activated receptor γ

Ppargc1a: Peroxisome proliferative activated receptor, gamma, coactivator 1 alpha

Ppargc1b: Peroxisome proliferative activated receptor, gamma, coactivator 1 beta

Prdm16: PR domain containing 16

PPRE: PPAR response element

P/S: Penicillin/streptomycin

qPCR: Quantitative PCR

Rb1: Retinoblastoma 1

ROSI: Rosiglitazone

Runx1t1: Runt-related transcription factor 1; translocated to, 1

RXR: Retinoid X receptor

Sirt3: Sirtuin 3

SH2: Src homology 2 domain

Src: Rous sarcoma oncogene

Srebf1: Sterol regulatory element binding transcription factor 1

Taz: Tafazzin

TNF-α: Tumor necrosis factor-alpha

Twist1: Twist homolog 1

UCP1: Uncoupling protein 1

UCP3: Uncoupling protein 3

WHO: World Health Organization

Wnt10b: Wingless related MMTV integration site 10b

LIST OF FIGURES

LIST OF SUPPLEMENTAL FIGURES

LIST OF TABLES

1.0 INTRODUCTION

1.1 Per- and polyfluoroalkyl substances (PFAS)

1.1.1 *Introduction to PFAS: Chemical properties and industrial uses*

Per- and polyfluoroalkyl substances (PFAS) is a group of synthetic chemicals widely used in various industrial and consumer products. The commercialization of PFAS chemicals became prevalent in the 1950s by companies such as 3M. Around this time, there was a close integration of the chemical industry into the military industry, emerging the "chemical century" (Agard-Jones, 2014; Langston, 2019). The widespread use of these chemicals across various industries stems from their valuable chemical properties. PFAS are unique due to the presence of carbon chains with carbon-fluorine (C-F) bonds. Due to the large electronegativity difference between fluorine and carbon, the bond between the two causes greater polarization, causing stronger electrostatic interactions, enhancing the chemical strength and thermal stability of PFAS, giving them the name "forever chemicals" (Liu *et al.,* 2019). Not only are these bonds highly stable, but also demonstrate hydrophobicity and lipophobicity. These properties together provide a highly valuable utilization of PFAS in many industrial and consumer products. In aqueous film-forming foam (AFFF), a type of firefighting foam, PFAS play a crucial role as surfactants, helping control and extinguish flammable liquid fires (Hall *et al.,* 2020; Rotander *et al.,* 2015). The hydrophobic and lipophobic properties of PFAS make them very useful in non-stick cookware (Ramirez Carnero *et al.,* 2015). PFAS have also introduced themselves into the cosmetic industry, in various makeup and skin care products to increase product durability (Shaikh *et al.,* 2023).

Different PFAS molecules are characterized by the presence of either a perfluorinated methyl group or perfluorinated methylene group, number of carbons, degree of fluorination and presence of other chemicals (Panieri *et al.*, 2022). Perfluoroalkyl substances can be split into different subgroups, most notably, perfluoroalkyl carboxylic acids (PFCAs) and perfluoroalkane sulfonic acids (PFSAs) (Buck *et al.*, 2011). PFCAs and PFSAs are sometimes described as longer-chained or shorter-chained. According to the Organization for Economic Cooperation and Development (OECD), PFCAs with 8 or more carbons and PFSAs with 6 or more carbons are considered longer-chained, whereas PFCAs with 7 or less carbons and PFSAs with 5 or less carbons are considered shorter-chained (OECD, 2013).

1.1.2 *Environmental persistence and contamination of PFAS*

Due to their status as "forever chemicals," PFAS exhibit high environmental persistence. Perfluorooctanoic acid (PFOA) and perfluorooctanesulfonic acid (PFOS), which are specific PFCAs and PFSAs, respectively, are the most detected and investigated PFAS in the environment (Wee & Aris *et al.*, 2023). PFAS contamination has been seen in surface waters and ground waters. Soils of AFFF-practicing sites were contaminated with PFOA and PFOS at high concentrations (up to 287 ng/g) (Filipovic *et al.*, 2015). Not only do these PFAS migrate in waters, but in sediments as well. Studies demonstrated that carbon-chain length and functional groups affected sediment-water partition coefficients (K_d), where higher K_d values were attributed to longer-chained PFAS, demonstrating these chemicals have a higher affinity to sediments relative to water, ranging from concentrations up to 30.9 ng/g (Wang *et al.*, 2022; Goodrow *et al.* 2020). Of more concern, PFAS contamination has been very prominent in

wastewaters. In Spain, 9.02 x 10^3 mg/day and 1.06 x 10^3 mg/day of PFOS and PFOA, respectively, were found in the daily sewage loads, which are being discharged into watercourses (main sources of drinking water for the area) (Campo *et al.*, 2014).

ChemSec identified that 12 chemical companies are responsible for majority of the global production of PFAS (3M, AGC, Arkema, Archoma, BASF, Bayer, Chemours, Daikin, Donyue, Honeywell, Merck and Solvay) (Chemsec, 2023). PFAS manufacturing plants have been identified in China, the United States of America, Germany and Belgium (Hughlett & Johnson, 2022; Jia *et al.*, 2023). In Canada, majority of PFAS hotspots are located in military bases because of their uses of AFFF to fight fuel fires, and in airports because of their uses for runway foaming (Weppler, 2023).

1.1.3 *Routes of PFAS exposure and associated health risks*

PFAS can enter the body through several routes. The dominant exposure pathway is through ingestion. PFAS has been found in main drinking water sources and they can accumulate in the food chain, leading to exposure through consumption of contaminated dairy products, seafoods, and meats (Campo *et al.*, 2014; Domingo, 2012). PFAS ingestion can also come indirectly from food packaging and cookware, by leaching into food during cooking or storage (Egeghy & Lorber, 2011). PFAS can also be absorbed into the body through inhalation. PFAS in consumer products can transfer into dust, which can result into exposure to PFAS-laden dust and airborne PFAS (Sukiene *et al.*, 2016; Björklund *et al.*, 2009). Another method for PFAS to enter the body through dermal absorption. Studies have observed dermal absorption from the use of handwipes (Poothong *et al.*, 2020; Poothong, *et al.*, 2019). Alarmingly, studies demonstrated the

estimated mean half-life for PFOA ranged from 1.5 to 5.1 years, and for PFOS, it ranged from 3.4 to 5.7 years (Rosato *et al.*, 2024). Given the multitude of pathways through which PFAS can enter the body and relatively long half-lives of PFAS, this presents significant concerns for human health.

PFAS has been associated with various human health risks. Liver has been claimed as a main target organ in short- and long-term exposure to PFAS (Knutsen *et al.*, 2018; Wang *et al.*, 2022; Chen *et al.*, 2024). Consistent population PFAS-altered liver enzyme findings have prompted investigations into non-alcoholic fatty liver disease (NAFLD) as a potential clinical outcome of PFAS exposure (Wang *et al.*, 2013). PFAS has also been implicated in human thyroid disease. Women exposed to concentrations of PFOA greater than 5.7 ng/mL demonstrated a correlation with hypothyroidism (Melzer *et al.*, 2010). PFAS exposure has also displayed negative reproductive effects in both men and women. For men, PFOA exposure had been shown to correlate with impairment of sperm motility and quality (Šabović *et al.*, 2020; Louis *et al.*, 2015). PFOS exposure has demonstrated decreased fertility rates for women (Fei *et al.*, 2009). While PFAS exposure can result in numerous negative impacts on humans, their influence on the endocrine system is often overlooked.

1.2 Endocrine disruption and metabolic disorders

1.2.1 *Endocrine disrupting chemicals (EDCs)*

The endocrine system is a complex network of glands and organs in the body that produce and release hormones into the bloodstream (Hiller-Sturmhöfel & Bartke, 1998). Exogenous chemicals known as endocrine disrupting chemicals (EDCs) have been recognized to disrupt the functions of the endocrine system. EDCs can cause sexual dysfunctions, reproductive

and developmental dysfunctions, which grow into detrimental results (Combarnous & Nguyen, 2019). EDCs have been seen to exert their effects on nuclear hormone receptors, such as androgen receptors (affected by phthalates), estrogen receptors (affected by bisphenol A), progesterone receptors (affected by perchlorates) etc.) (Huang *et al.*, 2020).

Metabolic disorders have been linked to many widely known factors, such as genetics, dietary patterns, and aging (Sun *et al.*, 2022). Interestingly, several studies have identified a relationship between EDCs and factors associated with increased risks of metabolic diseases. For example, clinical studies have shown the children with elevated body mass index and waist circumference also presented elevated urinary concentrations of phthalates (Trasande *et al.* 2013; Teitelbaum *et al.* 2012).

1.2.2 *Obesogens*

The Endocrine Society have defined EDCs as exogenous chemicals or mixture of chemicals that interfere with any aspect of hormonal action (Gore *et al.*, 2015). In a 2006 study, Grün and Blumberg proposed that a subgroup of endocrine disrupting chemicals, known as obesogens, can influence adipogenesis and be key factors that influence obesity (Grün & Blumberg, 2006). The obesogen hypothesis states that chemical pollutants can enhance adipocyte hyperplasia, promote adipocyte hypertrophy, disrupt appetite controls or alter homeostatic metabolic set points, can be defined as obesogens (Grün, 2010). PFAS have been implicated to have obesogen-like functions.

1.3 Understanding obesity and its health implications

1.3.1 *Obesity*

According to the World Health Organization (WHO), obesity is defined as an abnormal or excessive fat accumulation that presents a risk to health. In 2022, the WHO estimated that 1 in 8 people in the world were living with obesity (WHO, 2024). Their statistics demonstrated that 2.5 billion people that were 18 years and older were overweight, and 890 million were obese. 390 million people from ages 5-19 were overweight and 160 million were obese. 37 million children under the age of 5 were overweight. In Canada alone, 30% of male adults and 21% of female adults were considered obese (Government of Canada, 2024). Looking at these numbers, we can confirm that obesity is definitely a worldwide issue that requires a solution.

An important question to pose is, what are the possible causes of these increased number of cases of obesity. One of the primary causes of obesity is genetics. Genetic predisposition can have an influence on the regulation of the body's appetite and metabolism. Previous studies have shown that mothers with obesity are more likely to have obese children (Dabelea *et al.*, 2008). That being said, clinical intervention to cause maternal weight loss can reduce the risk of obesity in the offspring (Smith *et al.*, 2009). Another cause of obesity are dietary factors. The increased consumption calories, ultimately lead to weight gain. A 2021 study surveyed 1008 students and looked at the association between weight status and dietary factors, where results demonstrated that obese students had poor eating habits (i.e. fried foods, biscuits, cakes etc.) (Tunkara-Bah *et al.*, 2021).

Obesity is quantified with a body mass index greater than or equal to 30, which is calculated as weight (kg) over height (m) (Panuganti *et al.* 2022; Fruh, 2017). The obesity epidemic has become a significant health threat, resulting in higher morbidity/mortality rates, and an upsurge of costs to healthcare systems (D'Aiuto & Suvan, 2012). Obesity is associated with various diseases and conditions linked to increased mortality. These include Type 2 diabetes mellitus, cardiovascular diseases (CVD), hypertension, and certain types of cancer (Lin & Li, 2021).

1.3.2 *Type 2 diabetes*

Type 2 diabetes mellitus is defined by chronically elevated blood glucose and blood insulin (Westman, 2021). Insulin is a peptide hormone secreted by β cells of the pancreatic islets of Langerhans. It maintains normal blood glucose levels by facilitating cellular glucose uptake, promoting cell division and growth, and regulating carbohydrate, lipid and protein metabolism (Wilcox, 2005). Insulin facilitates cellular glucose uptake using the insulin signalling pathway. This pathway begins with the binding of insulin to the insulin receptor (IR). This induces conformational changes of the receptor, resulting in autophosphorylation and activation of receptor tyrosine kinases. This activation will enable the recruitment of insulin receptor substrate-1 (IRS1) (Kahn *et al.*, 2006). IRS1 will bind to the Src homology 2 domain (SH2) of phosphoinositide 3-kinase (PI3-K), activating PI3-K. PI3- K activates 3-phosphoinositide-dependent protein kinases-1 (PDK1), which results in the activation of protein kinase B (AKT). AKT phosphorylates various downstream target genes involved in the translocation of GLUT4 from the cytosol to the plasma membrane, stimulating glucose uptake (Wang *et al.*, 1999).

Elevated insulin in the body, seen in type 2 diabetes mellitus, is due to insulin resistance, where there is impaired biological response to insulin stimulation (Castro, 2022). The primary tissues which are involved in the development of insulin resistance are adipose tissue, liver and skeletal muscle (Freeman *et al.,* 2023). When there is an increased amount of blood glucose present, the pancreas will pump increased amounts of insulin to maintain blood glucose levels (CDC, 2024). When cells are insulin resistant, the pancreas will continue to secrete high concentrations of insulin, but will not be able perform its function, allowing for increase in blood glucose levels. This impairment in insulin secretion causes the development of β cell dysfunction, and these abnormalities of β cell function are key precursors of type 2 diabetes (Voight *et al.,* 2010).

1.4 Lipid metabolism

Lipid metabolism refers to the complex set of biochemical processes involved in the synthesis, storage, transport, and utilization of lipids (fats) in the body. Lipid metabolism maintains a continuous state of dynamic equilibrium, with ongoing synthesis of certain lipids and simultaneous oxidation of others (Gyami *et al.,* 2019). In the human body, lipids are essentials for their functional, structural and metabolic roles in cells and tissues (Alabdulkarim *et al,* 2012).

Lipid metabolism encompasses several key processes. Two important processes in lipid metabolism are lipogenesis and lipolysis. Lipogenesis is the process of synthesizing new fatty acids from non-lipid precursors (Saponaro *et al.,* 2015). Newly synthesized lipids and can be stored as energy, used for membrane biosynthesis or hormone synthesis (Coelho *et al.,* 2013; Bogdanov *et al.,* 2008; Payne & Hales, 2004). Insulin promotes lipogenesis primarily by

activating key enzymes involved in fatty acid synthesis and storage in adipose tissue and the liver (Yao *et al.*, 2023). Lipolysis, on the other hand, is the process of breaking down triglycerides into glycerol and free fatty acids (Edwards & Mohiuddin, 2023). Free fatty acids can then be released into the bloodstream where they can taken up by tissues for energy (Henderson, 2021). Insulin exerts an inhibitory effect on lipolysis by reducing cyclic adenosine monophosphate (cAMP) levels, which results in reduction in protein kinase A (PKA) activity (Degerman *et al.*, 1998).

1.5 Understanding adipose tissue and its functions

Adipose tissue is mainly composed of adipocytes, which function as calorie storage, accepting chemical energy in forms of fatty acids from the blood, where they will store them as triglycerides (Chen *et al.*, 2022; Church *et al.* 2012). Other functions of adipose tissue include regulating lipid mobilization/distribution in the body and producing many bioactive factors which communicate with other organs, regulating numerous different metabolic pathways (Luo & Liu, 2016). There are two primary types of adipose tissue: white adipose tissue and brown adipose tissue.

1.5.1 *Types of adipose tissue*

White adipose tissue, essential for energy storage, endocrine signaling, and insulin sensitivity, represents the predominant volume of adipose tissue in most mammals, including humans (Richard *et al*., 2020). *In vivo*, adipocyte morphology is characterized by a spherical shape, with a single, large lipid droplet occupying the majority of the cell volume, displacing the

organelles towards the cell's periphery. White adipocytes can expand to nearly 100 μm in diameter (Cinti, 2012).

Brown adipose tissue plays a vital role in non-shivering thermogenesis in mammals, a critical mechanism for survival in cold environments and the dissipation of excess energy (Lidell & Enerbäck, 2015; Carpentier *et al.*, 2023). The thermogenic function of brown adipocytes is attributed to their abundance of mitochondria, which harbor uncoupling protein 1 (UCP1), which acts as a proton transporter, disrupting adenosine triphosphate (ATP)-generating proton gradient, which leads to the dissipation of energy as heat, instead of ATP (de Sá *et al.*, 2017). These adipocytes get their brown hue from their increased density of mitochondria, which are rich in iron (Yook *et al.*, 2021). Brown adipocytes have an ellipsoidal shape, most-likely due to their high mitochondrial content (Cedikova *et al.*, 2016). Unlike white adipocytes, brown adipocytes, rather than having one unilocular lipid within the cell, they contain numerous smaller lipid droplets dispersed throughout the cell. Brown adipocytes typically grow from 15 to 50 μm in diameter (Cinti, 2012).

1.5.2 *Adipose tissue expansion and endocrine function*

Adipose tissue expansion occurs with hypertrophy (increasing adipocyte size) and hyperplasia (increasing number of adipocytes) (White *et al.*, 2017). Excess calories are first stored in the subcutaneous adipose depot, accomplished by hyperplasia (Horwitz & Birk, 2023). When hyperplasia reaches its limit and adipocytes have reached a certain size, hypertrophy takes place, increasing the risk of metabolic syndrome. The balance between hypertrophy and hyperplasia is a key factor in the metabolic outcome of obesity (Muir *et al.*, 2016). Adipose

tissue is well known for its function as energy storage in forms of fat, but its ability to secrete adipokines began its recognition as an endocrine organ. Adipose tissue has shown to secrete adipokines, such as adiponectin, tumor necrosis factor-alpha (TNF-α), leptin and many others (Coelho *et al.,* 2013; Khan & Joseph, 2014; Kelesidis, 2010; Galic *et al.* 2010). The adipocytes that make up the adipose tissue are formed through a process known as adipogenesis.

1.6 Adipogenesis

Adipogenesis is the proliferation and differentiation of undifferentiated mesenchymal cells into mature adipocytes (Ali *et al.,* 2013). This process includes the commitment step and the terminal differentiation step. The commitment step is where undifferentiated mesenchymal cells first differentiate into preadipocytes. When undifferentiated mesenchymal cells differentiate into preadipocytes, they have committed to the adipose lineage meaning they can only differentiate into mature adipocytes. When undergoing terminal differentiation, preadipocytes differentiate into mature lipid-filled adipocytes, which possess the required machinery for lipid synthesis.

1.6.1 *Transcriptional pathway orchestrating adipogenesis*

The differentiation process from preadipocytes into mature adipocytes involves a comprehensive network of transcription factors that are required for the expression of adipogenic proteins that induce mature adipocyte formation (Moseti *et al.,* 2016). Adipogenesis can be triggered by hormonal signals which activate G protein-coupled receptors (GPCRs), where they then activate adenylyl cyclase to catalyze the conversion of ATP to cAMP (Liu *et al.,* 2024). The

produced cAMP then bind and activate PKA. These activated PKA then phosphorylate various target proteins, one being cAMP response element-binding protein (CREB) (Siersbæk & Mandrup, 2011). The insulin signalling pathway can also lead to CREB phosphorylation. Phosphorylated CREB bind to the cAMP response element (CRE) in the promoter region of target genes, which include CCAAT/enhancer binding protein β and δ (C/EBPβ and C/EBPδ). These two will synergistically stimulate the expression of CCAAT/enhancer binding protein α (C/EBPα) and peroxisome proliferator-activated receptor γ (PPARγ), which are necessary for differentiation (Tanaka *et al.*, 1997). Glucocorticoids, such as dexamethasone, can also trigger adipogenesis by first bind glucocorticoid receptors (GRs), where the activated GR will translocate into the nucleus and bind glucocorticoid response elements in the promoter region of the PPARγ gene, directly inducing its expression or indirectly by inducing the expression of C/EBPβ and C/EBPδ.

PPARγ, known as the master regulator of adipogenesis, has been shown to promote mature adipocyte differentiation (El-Jack *et al.*, 1999). Along with PPARγ, C/EBPα is also another important adipogenic regulator and has been shown to be essential for adipogenesis both in culture and *in vivo.* Loss-of-function studies have shown that cells lacking PPARγ had greatly reduced expression of C/EBPα, and cells lacking in C/EBPα has greatly reduced expression of PPARγ (Kubota *et al.*, 1999; Wu *et al.*, 1999). This suggests that PPARγ and C/EBPα induce each others expression in a positive feedback loop, maintaining the differentiated state of mature adipocytes (Rosen *et al.*, 2002).

1.6.2 *Role of PPAR receptors in fatty acid metabolism*

PPARs are a group of ligand-activated transcription factors belonging to the nuclear receptor superfamily. These receptors play critical roles in regulation of various physiological processes, including metabolism, inflammation, and cell differentiation (Christofides *et al.*, 2021). The peroxisome proliferator-activated receptor (PPAR) nuclear receptor subfamily, include four main PPAR receptors: PPARγ, PPARα, PPARβ and PPARδ.

PPARγ can only regulate adipogenesis when activated by the binding of natural agonists (fatty acids) or synthetic agonists, such as antidiabetic thiazolidinediones (i.e. rosiglitazone (ROSI)) (Garin-Shkolnik *et al.*, 2014). Although ROSI is known for its role in regulating adipogenesis, it is used as medication for diabetic patients for improving their insulin sensitivity in peripheral tissue, promoting glucose uptake into cells, leading to improved blood glucose control (Quantanilla Rodriguez & Correa, 2022). Its pharmacological effects on glucose metabolism make it particularly useful for researchers investigating the links between adipogenesis, obesity and other metabolic disorders.

The activation of PPARα is associated with fatty acid oxidation. PPARα is known to be activated by the binding of natural fatty acids, or with the binding of synthetic agonist, for example, WY-14643. PPARα activation has also been involved in adipogenesis, in the presence of strong PPARα activators, however less efficiently than PPARγ-induced adipogenesis (Brun *et al.*, 1996).

Once activated, PPAR receptors (either PPARγ or PPARα) heterodimerize with retinoid X receptor (RXR), and translocate into the nucleus to bind to specific DNA sequences, known as PPAR response element (PPRE) (Mangelsdorf *et al.*, 1995; Chandra *et al.* 2008). RXR binding

by PPAR receptors facilitates their nuclear translocation, enhances their DNA binding affinity, and increases their transcriptional activity, ultimately regulating the expression of target genes (Krey *et al.,* 1993; IJpenberg *et al.,* 1997). The binding of the PPAR-RXR heterodimer to specific PPRE sequences facilitate the assembly of the transcriptional machinery, leading to activation of target gene transcription. PFOA and other PFAS have demonstrated to bind and activate both PPARγ and PPARα (Evans *et al.,* 2022).

1.6.3 *3T3-L1 preadipocyte cell model*

Differentiation of 3T3-L1 preadipocytes into mature adipocytes is one of the most commonly used *in vitro* models to study adipogenesis. The 3T3-L1 cell line was developed from disaggregated 17-19 day old Swiss 3T3 mouse embryos, where in appropriate conditions and exposure to adipogenic stimuli, can acquire adipocyte-like phenotype (Ruiz-Ojeda *et al.,* 2016). 3T3-L1 differentiation is caused by stimulation with insulin, dexamethasone and 1-methyl-3-isobutyl-xanthine (IBMX). Insulin stimulates cells to take up glucose and store energy in forms of triglycerides (Jakab *et al.,* 2021). Dexamethasone binds and activates the GR. The activated GR translocates to the nucleus and bind to specific DNA sequences found in the promoter region of target genes, known as GRE. This binding induces the expression of C/EBPδ, which induces expression of C/EBPα. IBMX is a competitive, nonselective phosphodiesterase inhibitor. Phosphodiesterase is responsible for the break down of cAMP, therefore its inhibition raises intracellular cAMP, which ultimately leads to PKA activation. PKA signalling pathway is shown to promote the transcriptional activation of PPARγ, ultimately promoting adipogenesis (Kim *et al.,* 2010). After introducing cells with adipogenic hormones, differentiating preadipocytes undergo mitotic clonal expansion (MCE), where they re-enter the cell cycle for two rounds of

cell division, where an irreversible commitment to adipocyte differentiation occurs (Hishida *et al.*, 2009). Some studies claim that if MCE does not occur, expression of adipogenic transcription factors and regulators will not occur, ultimately blocking differentiation (Tang *et al.*, 2003). However, a study by Qiu *et al.* demonstrated that in the absence of insulin, adipogenesis did occur without MCE (Qiu *et al.*, 2001). The 3T3-L1 cell line is an already established cell line, making it easier and more cost efficient to use to study adipogenic differentiation in comparison to freshly isolated cells (Poulos *et al.*, 2010).

This differentiation process can be confirmed by assessing the expression of adipogenic markers. Some of these markers include fatty acid binding protein 4 (*FABP4*), also known as adipocyte protein 2 (*aP2*), lipoprotein lipase (*LPL*), and *perilipin*. *FABP4* is involved in the regulation of glucose and lipid metabolism, especially in adipocytes (Furuhashi *et al.*, 2014). *LPL* mediates the release of fatty acids from lipoproteins in the blood stream to the adipocyte cell surface to undergo diffusion-based transport into the adipocyte. *Perilipin* has been seen to form a coat on adipocyte lipid droplets, protecting them until lipases are transported from the cytoplasm, which is required to break down the fat storage.

1.6.4 *Known effects of PFAS on 3T3-L1 preadipocyte differentiation*

A study by Yamamoto *et al.* demonstrated that PFOA at 100 μM increased PPARγ activation in 3T3-L1 preadipocytes, suggesting that PFOA at high concentrations can act as a PPARγ agonist (Yamamoto *et al.*, 2015). When investigating differentiation of 3T3-L1 preadipocytes, this study indicated that PFOA treatment enhanced differentiation and lipid

accumulation at this concentration. Studies have also shown that mRNA levels of PPARγ, C/EBPα, aP2, and *LPL* were upregulated at higher concentrations of PFOA (Ma *et al.,* 2018).

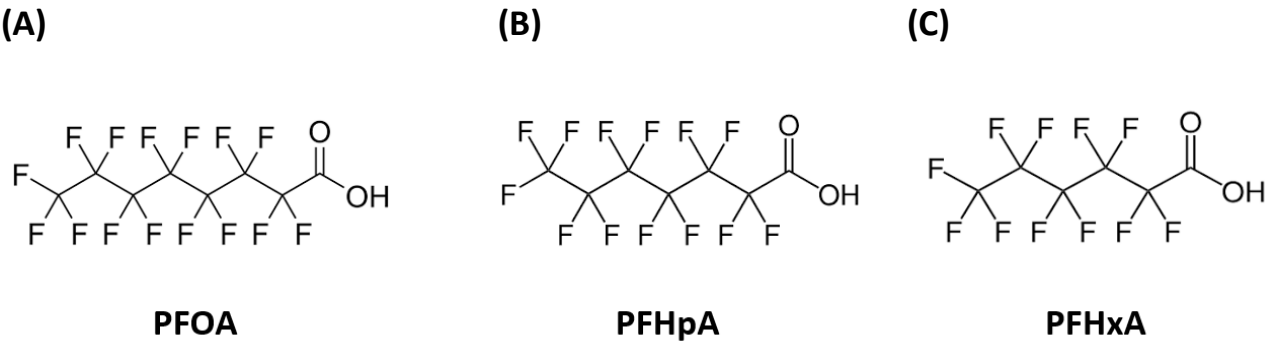

Figure 1. Chemical structures of longer and shorter-chained PFCAs. (A) PFOA, (B) PFHpA and (C) PFHxA.

RATIONALE

There are numerous implications of perfluorinated carboxylic acids (PFCAs) on human health, but their effects on adipogenesis remain largely unexplored and necessitate further research. The most abundant PFCA, PFOA, has been shown to induce the expression of adipogenic markers and enhance lipid accumulation in 3T3-L1 preadipocytes (Yamamoto *et al.*, 2015). However, the shorter-chained PFCAs, such as perfluoroheptanoic acid (PFHpA) and perfluorohexanoic acid (PFHxA), which are often used as substitutes for longer-chained PFCAs like PFOA, have not been extensively studied in the context of adipogenesis. Given the structural similarities between these substitutes and PFOA, it is plausible that they might exhibit similar effects on adipogenesis. This research area needs more investigation to elucidate the potential impacts of shorter-chained PFCAs on adipogenesis and to uncover the mechanisms through which PFCAs might induce adipogenesis.

I hypothesize that shorter-chained PFCAs, specifically PFHpA and PFHxA, may influence adipogenesis in a manner similar to PFOA. To test this hypothesis, I proposed the following specific aims:

SPECIFIC AIMS:

Aim 1: Investigate the effects of the shorter-chained PFCAs (PFHpA and PFHxA) on adipogenesis.

Aim 2: Investigate the mechanism by which these chemicals may induce adipogenesis.

2. MATERIALS AND METHODS

2.1 Alamar Blue Assay

An Alamar Blue Assay was performed to test the cell viability of 3T3-L1 cells when exposed to PFOA (0-100 μM), PFHpA (0-100 μM) or PFHxA(0-100 μM). 25,000 cells were plated per well in a 96-well plate (Corning Incorporated, Corning, New York, United States) and incubated in 10% CO_2, at 37°C for 24 hours. Media was then aspirated and 200 μL of chemical treatments were added to the wells, and incubated in 10% CO_2, at 37°C for 48 hours. 100 μL of media was removed from each well and 25 μL of CellTiter-Blue reagent (Promega, Madison, Wisconsin, United States) was added to each well. Cells were incubated in 10% CO_2, at 37°C for 1 hour, then fluorescence was read in a Fluostar Optima plate reader (BMG, Ortenberg, Germany) to read fluorescence at 530 nm/590 nm (excitation/emission).

2.2 Cell Culture and Differentiation

2.2.1 *3T3-L1 cell maintenance*

3T3-L1 mouse embryonic fibroblasts were obtained from the American Type Culture Collection (ATCC, Manassas, Virginia). These cells in dimethylsulfoxide (DMSO) (Sigma-Aldrich, St. Louis, Missouri, United States) were directly stored in liquid nitrogen. 3000 cells/cm^2 were thawed, then plated in a 10cm petri dish containing 10 mL of maintenance media: Dulbecco's modified Eagle's medium low glucose (DMEM low glucose) (Wisent Inc., Saint-

Jean-Baptiste, Quebec, Canada) supplemented with 10% bovine calf serum (BCS) (ATCC), pre-warmed to 37°C. Cells were then incubated in 10% CO_2, at 37°C overnight. Cells were replenished with fresh maintenance media the following day, preventing cell death which might occur from the presence of 5% DMSO of the cells taken from the liquid nitrogen. After replenishment, cells were then incubated in 10% CO_2, at 37°C. Once cells were 60-70% confluent, cells were split into multiple plates. To split plates, media was aspirated, then replaced with 10 mL of phosphate-buffered saline (PBS). PBS was removed and replaced with 1 mL 0.5% trypsin-ethylenediamine tetraacetic acid (EDTA) (Life Technologies Corporation, Carlsbad, California, United States) and incubated in 10% CO_2, at 37°C, for 1-2 minutes, to detach cells from dish. To prevent cell death from prolonged trypsin exposure, trypsin was deactivated with the addition of the appropriate amount of maintenance media. Lifted cells were then distributed amongst 10 cm petri dishes.

2.2.2 *3T3-L1 preadipocyte differentiation*

Cells were grown until 80% confluence, then seeded into 6-well plates. Cells were left to reach 100% confluence (day -2). Cells were left for another two days after reaching 100% confluence (day 0). On day 0, maintenance media was removed and replaced with differentiation media (DMEM low glucose supplemented with 10% fetal bovine serum (FBS) (Wisent Inc.) and 1% penicillin/streptomycin (P/S) (Wisent Inc.). Differentiation was induced with 0.5 mM IBMX (Sigma-Aldrich), 100 nM insulin (Roche Applied, Penzberg, Germany) and one of the following chemicals: ROSI (200 nM) (Sigma-Aldrich), WY-14643 (20 μM) (Cayman Chemical Company, Ann Arbor, Michigan, United States), PFOA (0-100 μM), PFHpA (0-100 μM), or PFHxA (0-100 μM) (Sigma-Aldrich). Medium was replaced every two days throughout the 6-day (for RT-

qPCR) or 8-day (lipid accumulation) differentiation process. Cells were treated with IBMX and ROSI from day 0-2, whereas with insulin, WY-14643, PFOA, PFHpA and PFHxA, cells were treated from day 0-6/8.

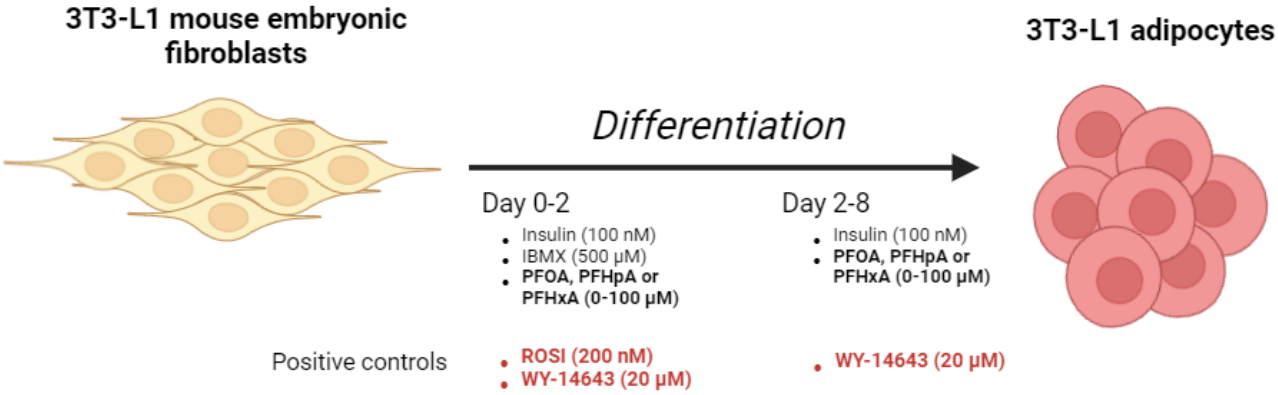

Figure 2. Timeline of 3T3-L1 adipocyte differentiation. 3T3-L1 preadipocytes were grown to 100% confluence. Two days post-confluence (Day 0), cells were then treated as in with either the positive controls (200 nM ROSI or 20 µM WY-14643) or with PFOA, PFHpA or PFHxA from 0-100 µM. Expression of mature adipocyte makers and genes involved in fatty acid oxidation were assessed on Day 6 for mRNA. On Day 8, lipid accumulation was assessed. Figure was created using BioRender.

2.3 Real-Time Quantitative PCR (qPCR) Reaction

2.3.1 *RNA extraction and purification*

3T3-L1 adipocytes were harvested on day 6 of differentiation. Media was aspirated replaced with 350 µL of lysis buffer (RLT buffer (QIAGEN, Mississauga, ON, Canada), 1% β-mercaptoethanol). Cells on the wells were scraped using Falcon™ Cell Scrapers, then homogenized with a needle syringe ready for purification and transferred to 1.5 mL Eppendorf tubes (RNA extraction can be performed or lysed cells can be stored at -80°C)

RNA extraction and purification was performed using the RNeasy Mini Kit as per the manufacturer's instruction (QIAGEN). Briefly, 350 µL of 70% ethanol was added to lysate and pipette mixed (precipitating nucleic acids out of the solution). The 700 µL solution was then transferred to a RNeasy spin column placed in a 2 mL collection tube (QIAGEN), then centrifuged at 12,000 rpm for 30 seconds. The flow through was discarded and 350 µL of RW1 Buffer (QIAGEN) was added to the column, then centrifuged at 12,000 rpm for 30 seconds. A DNA digestion was then performed by adding 80 µL DNAse solution (12% DNase, 88% RDD Buffer), and incubating it for 15 minutes at room temperature. 350 µL of RW1 was added on top of the DNAse solution, then centrifuged at 12,000 rpm for 30 seconds. The flow through was discarded, the collection tube was changed, then 500 µL of RPE Buffer (QIAGEN) and centrifuged at 12,000 rpm for 30 seconds. This step was repeated a second time. A dry centrifuge of the column was done for 2 minutes to ensure minimal ethanol carryover during RNA elution. The column was then transferred to a new 1.5 mL Eppendorf tube and 50 µL of RNAse-free

water was added to the column and centrifuged at 10,000 rpm for 1 minute. The RNA elution was stored at -80°C.

2.3.2 *cDNA synthesis*

RNA was quantified and a quality analysis was performed using the DS-11 Spectrophotometer (DeNovix, Wilmington, Delaware, USA). The spectrophotometer was first blanked using 1 µL of RNAse-free water. Then, the concentration of 1 µL of total RNA was measured.

cDNA was synthesized using 500 ng of total RNA, the appropriate amount of ddH_2O, 4 µL of iScript Buffer 5X (BioRad, Hercules, California, United States) and 1 µL reverse transcriptase (total reaction is 20 µL). cDNA was synthesized using CFX96 Real-Time System C1000 Thermal Cycler (BioRad) at the recommended cycling conditions.

2.3.3 *Real-time qPCR analysis*

Each qPCR reaction was performed using 4 µL of cDNA and 6 µL of qPCR mastermix (5 µL of SsoFast EvaGreen qPCR Supermix (BioRad), 0.5 µL of nuclease-free water, 0.25 µL forward primer of appropriate gene and 0.25 µL of reverse primer of appropriate gene), in triplicates, in 96-well plates (BioRad). qPCR reactions were performed using CFX96 Real-Time System C1000 Thermal Cycler at the recommended cycling conditions. Transcriptional expression levels of *FABP4. LPL*, *perilipin*, acyl-CoA oxidase 1 (*ACOX1)*, uncoupling protein 3

(*UCP3)*, and carnitine palmitoyltransferase 1B *(CPT1b)*, normalized to β-*actin* levels. All primers use were listed in the appendix (Table 1).

2.4 Luciferase Assays

Luciferase assays of PPARγ and PPARα were performed using the Human Peroxisome Proliferator-Activated Receptor Gamma Reporter Assay System and the Human Peroxisome Proliferator-Activated Receptor alpha Reporter Assay System, respectively (Indigo Biosciences, State College, Pennsylvania, United States), as per the manufacturer's instructions, described below.

2.4.1 *PPARγ luciferase assay*

Compound Screening Media (CSM) (Indigo Biosciences) was pre-warmed to 37°C. Using CSM, treatments were made with a 2X concentration. ROSI was used as the positive control for this assay.

Cell recovery medium (CRM) (Indigo Biosciences) was pre-warmed to 37°C. PPARγ reporter cells (Indigo Biosciences) were rapid thawed immediately by dispensing 10 mL of CRM into tube of frozen cells. The tube was then placed in a 37°C water bath for 5-10 minutes. Reporter cells were inverted several times then transferred to a media reservoir. 100 µL of cells per well were immediately dispensed into a white 96-well plate with flat bottoms (Indigo Biosciences). 100 µL of treatments were dispensed into appropriate wells. The plate was then incubated in 5% CO_2, at 37°C, for 22-24 hours.

Detection substrate and detection buffer (Indigo Biosciences) was equilibrated to room temperature, then inverted several times. Detection Buffer was directly added to the Detection Substrate vial, generating the Luciferase Detection Reagent (LDR). Media was discarded from white 96-well plate, and 100 µL of LDR per well was added was incubated for at least 5 minutes at room temperature.

A "plate shake" was administered manually for 5 seconds then placed in a Glomax 96 microplate Luminometer (Promega) and luminescence was quantified.

2.4.2 *PPARα luciferase assay*

Two tubes of CRM (Indigo Biosciences) was pre-warmed to 37°C. PPARα reporter cells (Indigo Biosciences) were rapid thawed immediately by dispensing 19 mL of CRM (9.5 mL per CRM tube) into tube of frozen cells. The tube was then placed in a 37°C water bath for 5 minutes. Reporter cells were inverted several times then transferred to a media reservoir. 200 µL of cells per well were immediately dispensed into a white 96-well plate with flat bottoms (Indigo Biosciences). The plate was then incubated in 5% CO_2, at 37°C, for 4-6 hours.

Near the end of the pre-incubation, CSM (Indigo Biosciences) was pre-warmed to 37°C, treatments were made with 1X concentration. GW7647 was used as the positive control for this assay.

Media was discarded from white 96-well plate, and 200 µL of treatments were dispensed into appropriate wells. The plate was then incubated in 5% CO_2, at 37°C, for 22-24 hours.

Detection substrate and detection buffer (Indigo Biosciences) was equilibrated to room temperature, then inverted several times. Detection Buffer was directly added to the Detection Substrate vial, generating the LDR. Media was discarded from white 96-well plate, and 100 µL of LDR per well was added was incubated for 5-10 minutes at room temperature.

A "plate shake" was administered manually for 5 seconds then placed in a Glomax 96 microplate Luminometer (Promega) and luminescence was quantified.

2.5 Lipid Quantification and Imaging

3T3-L1 cell were differentiated for 8 days in black 96-well with clear bottoms (PerkinElmer) before staining. After 8 days, media was aspirated, and cells were washed twice with PBS, then fixed with 100 µL of 10% formalin (Electron Microscopy Sciences, Hatfield, Pennsylvania, United States) per well, for 30 minutes at room temperature. Formalin was removed and washed twice with 100 µL PBS, ready for staining.

PBS was removed and replaced with 100 µL PBS with 0.2% TritonX-100 (Sigma-Aldrich) for permeabilization. Cells were permeabilized for 15 minutes at room temperature, then removed and washed with 100 µL PBS twice.

Cells were stained with 100 µL of staining solution (1 µg/mL DAPI and 1 µg/mL BODIPY493 (ThermoFischer Scientific, Waltham, Massachusetts, United States) in PBS) for 30 minutes, at room temperature, protected from light. Stain was removed and cells were washed with 100 µL PBS 3 times, then sealed in parafilm, and wrapped in tinfoil for storage at 4°C, until ready for imaging.

Cells were imaged and lipid accumulation was quantified using the OPERA Phenix High-Content Screening System (PerkinElmer).

2.6 Mouse Adipogenesis RT^2 Profiler PCR Array

Mouse adipogenesis RT^2 Profiler PCR Arrays were purchased from QIAGEN, and PCR reactions were performed using their protocol.

2.6.1 *RT^{2}First Strand Kit cDNA synthesis*

Reagents in the RT^2 First Strand Kit (QIAGEN) were thawed. Genomic DNA mix was made with 500 ng RNA, appropriate amount of RNAse-free water, and 2 µL Buffer GE (total reaction is 10 µL). The genomic DNA mix was incubated at 42°C for 5 minutes, immediately transfer on ice for at least 1 minute. While on ice, reverse-transcription mix is made using 4 µL of 5X Buffer BC3, 1 µL Control P2, 2 µL of RE3 Reverse-transcriptase mix and 3 µL of RNAse-free water (total reaction is 10 µL). The reverse-transcriptase mix was added to the 10 µL of genomic elimination DNA mix and pipette mixed. Reaction was then incubated at 42°C for 15 minutes, then the reaction is immediately stopped by incubation at 95°C for 5 minutes. 91 µL of RNAse-free water is added to the reaction, pipette mixed, then was stored at -20°C.

2.6.2 *Real-time PCR for RT^{2}profilier PCR Array*

RT^2 SYBR Green Mastermix (QIAGEN) and cDNA reaction was thawed. 1350 µL of SYBR Green Mastermix, 1248 µL RNAse-free water and 102 µL of the cDNA synthesis reaction

was added and mixed in a loading reservoir (total volume is 2700 µL). Using a multichannel pipette, 25 µL per well of the mix was added to RT^2 Profiler PCR Array (QIAGEN). Plate was sealed using Optical Thin-Wall 8-cap Strips (QIAGEN), then centrifuged for 1 minute at 1000 g. Real-time PCR reactions were performed using CFX96 Real-Time System C1000 Thermal Cycler at the recommended cycling conditions.

2.7 Statistical Analysis

P-values for luciferase data, qPCR data and lipid accumulation data were calculated with the GraphPad Prism 10.2.1 software using a one-way or two-way ANOVA followed by Dunnett's multiple comparisons test or Tukey's multiple comparisons test, respectively, to determine statistical significance between multiple means. P-values for RT^2 profiler PCR Array data was calculated with Qiagen's data analysis software, GeneGlobe, using a Student's t-test (two-tail distribution and equal variances between the two samples).

3. RESULTS

3.1 Analyzing the cell viability of 3T3-L1 preadipocytes in the presence of PFCAs (PFOA, PFHpA and PFHxA) at varying concentrations

Before assessing the effects of PFCAs on 3T3-L1 cells, the cell viability of these cells in the presence of PFOA, PFHpA or PFHxA at concentrations from 0-100 µM was determined by performing Alamar Blue assays.

Results demonstrated that PFOA, PFHpA and PFHxA from concentration 0-100 µM weren't cytotoxic to 3T3-L1 preadipocytes (Figure 3).

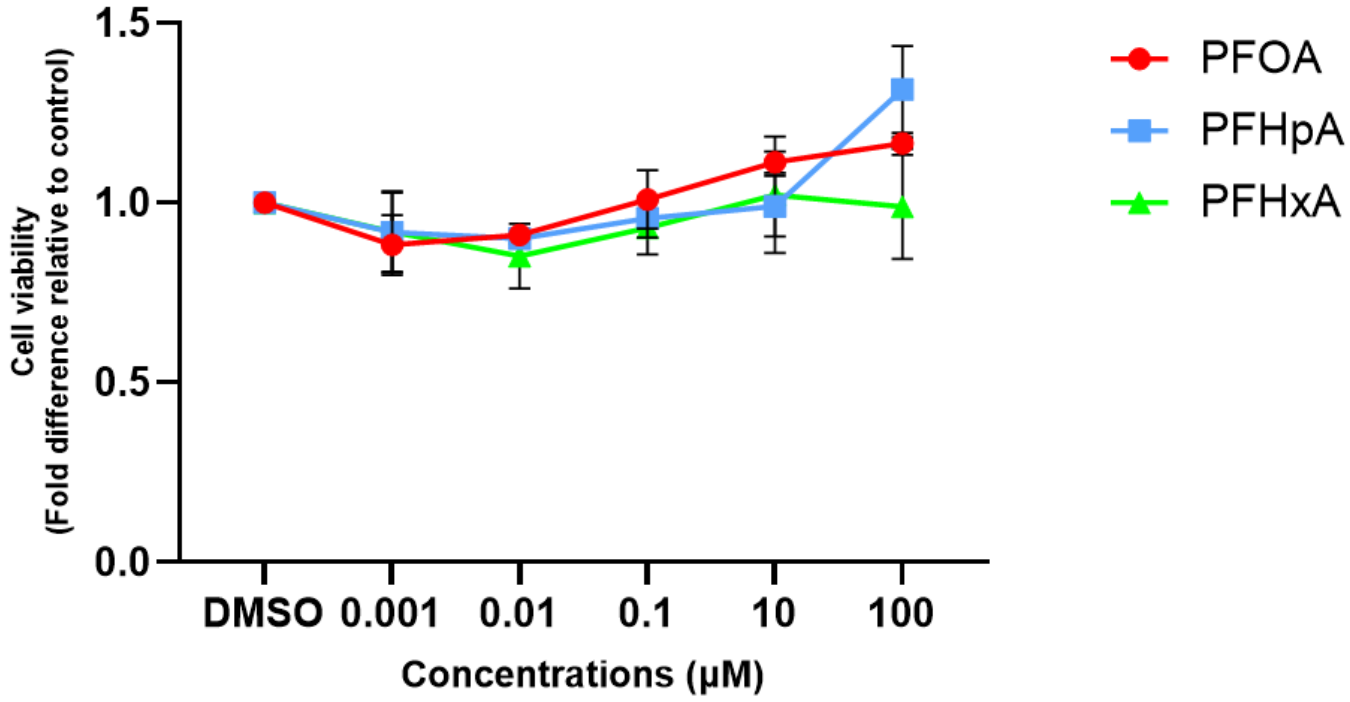

Figure 3. Effects of PFOA, PFHpA and PFHxA on 3T3-L1 cell viability. 3T3-L1 preadipocytes were treated with DMSO, PFOA (0-100 µM), PFHpA (0-100 µM), or PFHxA (0-100 µM). Cell viability was assess using CellTiter-Blue and fluorescence was measured at 530 nm/590 nm (excitation/emmision). Data was represented by the mean fold change ± standard error of mean (SEM).

3.2 Transcriptional expression analysis of adipogenic markers in the presence of PFOA, PFHpA or PFHxA

Adipogenic markers are specific genes which are expressed during the process of adipogenesis. Some of the main adipogenic markers, include *FABP4, LPL* and *perilipin*. PFAS-treated cells have been shown to increase the expression of key adipogenic markers. A Yamamoto *et al.* study demonstrated that PFOA induced adipogenesis as illustrated by the increased expression of adipogenic markers (Yamamoto *et al.,* 2015). This study induced adipogenesis with PFOA with the adipogenic inducers insulin, IBMX, and the glucocorticoid, dexamethasone. Our study lacked the presence of dexamethasone, as previously in our lab, we were able to induce adipogenesis solely with insulin, IBMX and ROSI (Peshdary *et. al*., 2019). In PFAS-treated 3T3-L1 cells, we analyzed the expression of three adipogenic markers: *FABP4, LPL* and *perilipin*.

3.2.1 *PFOA and PFHpA-treated cells, but not PFHxA treatments up-regulate the mRNA levels of FABP4 in 3T3-L1 preadipocytes*

In order to test the adipogenic potential of other PFAS, we looked at the expression of *FABP4* in PFAS-treated cells. PFOA and PFHpA-treated 3T3-L1 preadipocytes exhibited significant increased expression of *FABP4* at 100 µM, relative to control (Figure 4A). Specifically, PFOA-treated cells at 100 µM showed an 8.4-fold increase in *FABP4* expression relative to the solvent control, while PFHpA treatments at the same concentration demonstrated a 7.4-fold increase in *FABP4* expression relative to the solvent control. Treatment with 0-50 µM PFOA or PFHpA did not increase *FABP4* expression in the 3T3-L1 cells. PFHxA-treated cells

did not demonstrate any change in *FABP4* expression. Significant differences were seen in the expression of *FABP4* between the PFOA-treated cells and PFHxA treatments, but no significant changes were seen between the PFOA treatments and PFHpA-treated cells. Cell treated with the positive controls, ROSI at 200 nM and WY-14643 at 20 µM, showed substantial increases of 53.6-fold and 23.8-fold, respectively, in *FABP4* expression relative to the solvent control (Figure 4B).

3.2.2 *PFOA, PFHpA and PFHxA-treated cells up-regulate the mRNA levels of LPL in 3T3-L1 preadipocytes*

To test the adipogenic potential of other PFAS, we also looked at the expression of *LPL* in PFAS-treated cells. All three PFCAs treatments exhibited significant expression of *LPL* at 100 µM in 3T3-L1 preadipocytes (Figure 4C). Specifically, PFOA-treated cells at 100 µM showed a 2.2-fold increase in *LPL* expression relative to the solvent control, while PFHpA-treated cells at the same concentration demonstrated a 2.3-fold increase, and PFHxA-treated cells demonstrated a 2.0-fold increase in *LPL* expression relative to the solvent control. PFOA, PFHpA and PFHxA-treated cells did not increase *LPL* expression in cell at lower concentrations (0-50 µM). Additionally, cells treated with the positive controls, ROSI at 200 nM and WY-14643 at 20 µM, displayed substantial increases of 12.0-fold and 5.00-fold, respectively, relative to the solvent control (Figure 4D).

3.2.3 *PFOA, PFHpA and PFHxA-treated cells up-regulate the mRNA levels of perilipin in 3T3-L1 preadipocytes*

Another adipogenic marker which is expressed highly in mature adipocytes is *perilipin,* therefore we assessed the effects of PFAS on the mRNA expression levels of this gene. All three PFCA treatments tested significantly increased the expression levels of *perilipin* mRNA at 100 µM in 3T3-L1 preadipocytes (Figure 4E). Specifically, PFOA-treated cells at 100 µM showed a 5.3-fold increase in *perilipin* expression relative to the solvent control, while PFHpA-treated cells at the same concentration demonstrated a 4.7-fold increase, and PFHxA-treated cells demonstrated a 2.9-fold increase in *perilipin* expression relative to the solvent control. PFOA-treated cells did not exhibit significant change in *perilipin* from concentration 0-25 µM, whereas for PFHpA and PFHxA-treated cells, no significant change was presents from 0-50 µM. Significant differences were seen in the expression of *perilipin* between the PFOA-treated cells and PFHxA-treated cells, specifically a 2.4-fold increase in *perilipin* expression in PFOA-treated cells relative to PFHxA-treated cells. No significant differences were seen between the PFOA-treated cells and PFHpA-treated cells. Additionally, cells treated with the positive controls, ROSI at 200 nM and WY-14643 at 20 µM, displayed substantial increases of 27.3-fold and 11.0-fold, respectively, in *perilipin* mRNA expression levels, relative to the solvent control (Figure 4F).

(A)

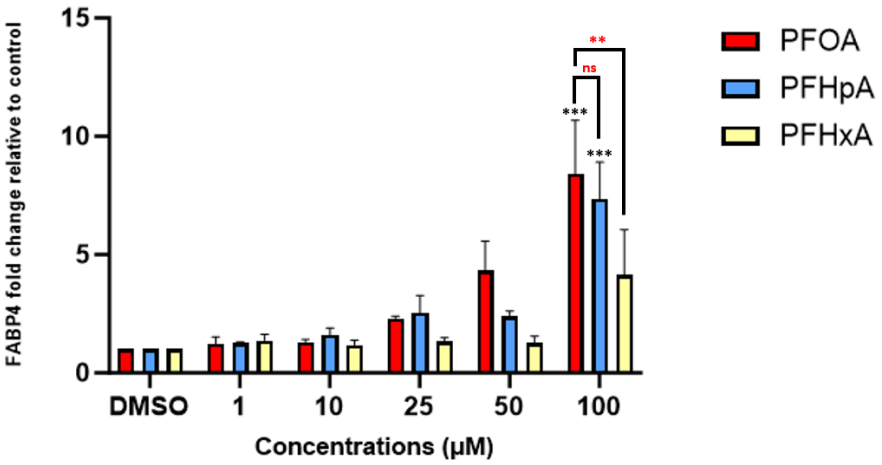
FABP4 fold change relative to control
15
10
5
0
**
ns
***
***
DMSO
1
10
25
50
100
Concentrations (μM)
PFOA
PFHpA
PFHxA

(B)

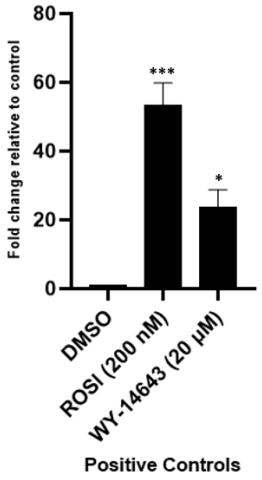
Fold change relative to control
80
60
40
20
0
***
*
DMSO
ROSI (200 nM)
WY-14643 (20 μM)
Positive Controls

(C)

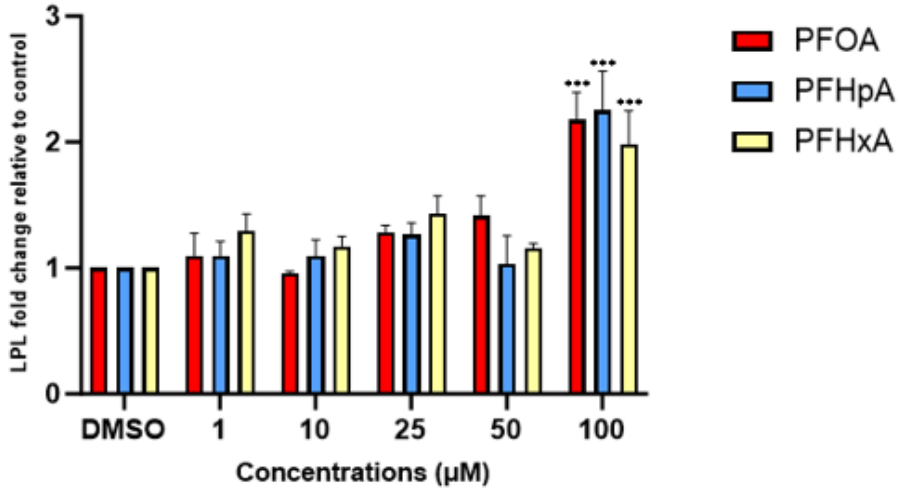
LPL fold change relative to control
3
2
1
0
***
***
***
DMSO
1
10
25
50
100
Concentrations (μM)
PFOA
PFHpA
PFHxA

(D)

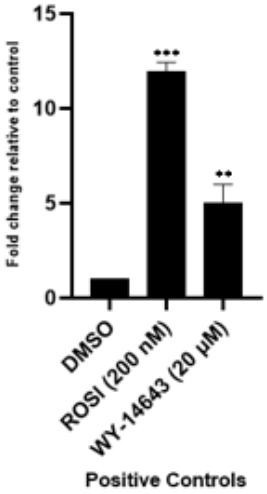
Fold change relative to control
15
10
5
0
***
**
DMSO
ROSI (200 nM)
WY-14643 (20 μM)
Positive Controls

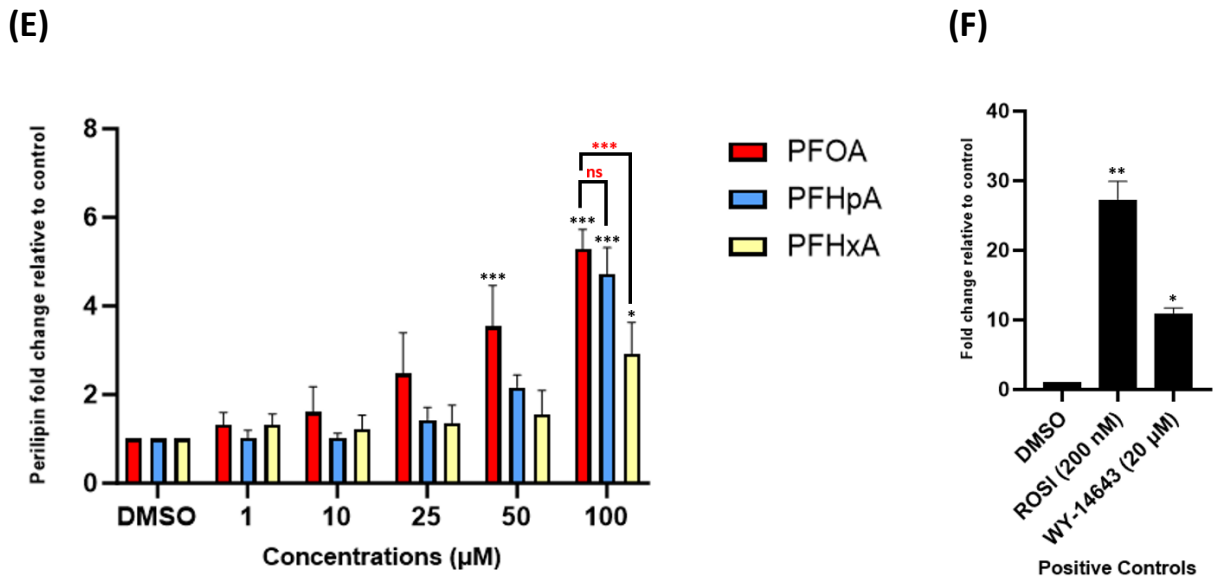

Figure 4. Transcriptional expression analysis of adipogenic markers of 3T3-L1 preadipocytes treated with PFOA, PFHpA and PFHxA from concentrations ranging between 0-100 µM. 3T3-L1 preadipocytes were induced to differentiate in 6-well plates for 6 days in the presence of 500 µM IBMX (day 0-2), 100 nM insulin (day 0-6) and one of the three test PFAS chemicals (0-100 µM). Positive controls were treatments with 200 nM ROSI or 20 µM WY-14643. The solvent control used was DMSO. On day 6, cells were harvested, and RNA was isolated. qPCR analysis was used to assess the expression levels of three adipogenic markers: (A) *FABP4*, (B) *LPL* and (C) *perilipin.* Levels were normalized to *β-actin* levels and expressed as fold over solvent control. Data was represented the mean fold change ± standard error of mean (SEM) where *P<0.05, **P<0.01, ***P<0.001 relative to vehicle control, and ns (non-significant), *P<0.05, **P<0.01, ***P<0.001 relative to PFOA-treated cells, using a two-way ANOVA or one-way ANOVA followed by Tukey's multiple comparisons test or Dunnett's multiple comparisons test, respectively.

3.3 Lipid accumulation in 3T3-L1 preadipocytes treated with PFOA, PFHpA or PFHxA from 0-100 µM

As the transcriptional expression analysis demonstrated increased expression of adipogenic markers at higher concentrations of PFOA, PFHpA and PFHxA, this led to the conclusion that treatment with these three chemicals are involved in promoting adipogenesis. To confirm this statement, high-throughput imaging was used to visualize and quantify lipid accumulation within 3T3-L1 preadipocytes treated with PFOA, PFHpA or PFHxA from 0-100 µM.

3.3.1 *PFOA, PFHpA or PFHxA at higher concentrations increased lipid accumulation in 3T3-L1 preadipocytes*

All three PFCA-treatments exhibited significant increases in lipid accumulation at higher concentrations (Figure 5B). Specifically, PFOA-treated cells at the concentrations of 50 µM and 100 µM showed a 2.2-fold and 2.6-fold increase in lipid accumulation relative to the solvent control, respectively. PFHpA-treated cells at 100 µM demonstrated a 2.9-fold increase, while PFHxA-treated cells at concentrations of 50 µM and 100 µM displayed a 2.5-fold and 2.4-fold increase in lipid accumulation relative to the solvent control, respectively. Additionally, treatment with the positive controls, ROSI at 200 nM and WY-14643 at 20 µM, demonstrated increases of 3.6-fold and 2.7-fold, respectively, in lipid accumulation relative to the solvent control (Figure 5C).

(A)

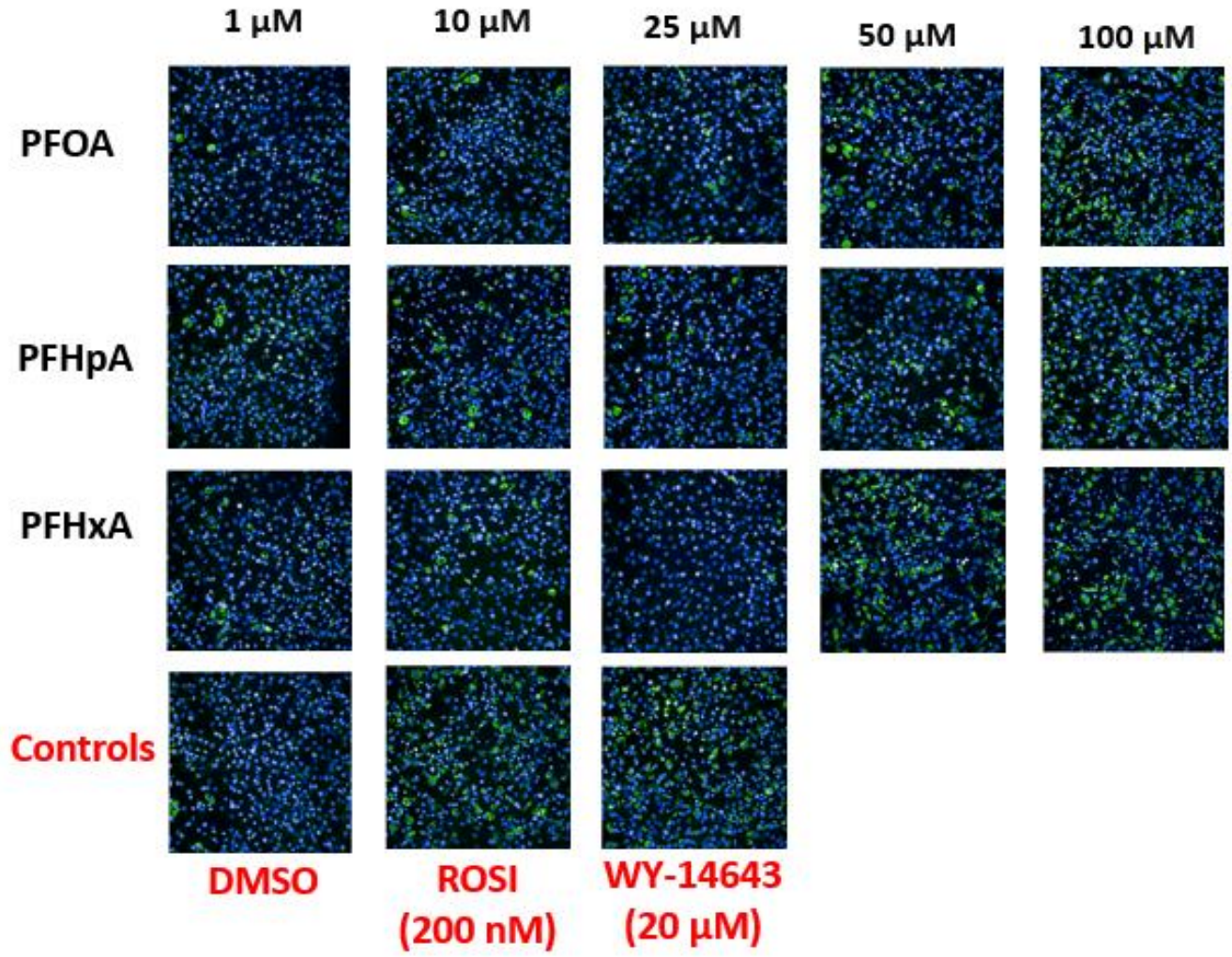
1 µM
10 µM
25 µM
50 µM
100 µM
PFOA
PFHpA
PFHxA
Controls
DMSO
ROSI
(200 nM)
WY-14643
(20 µM)

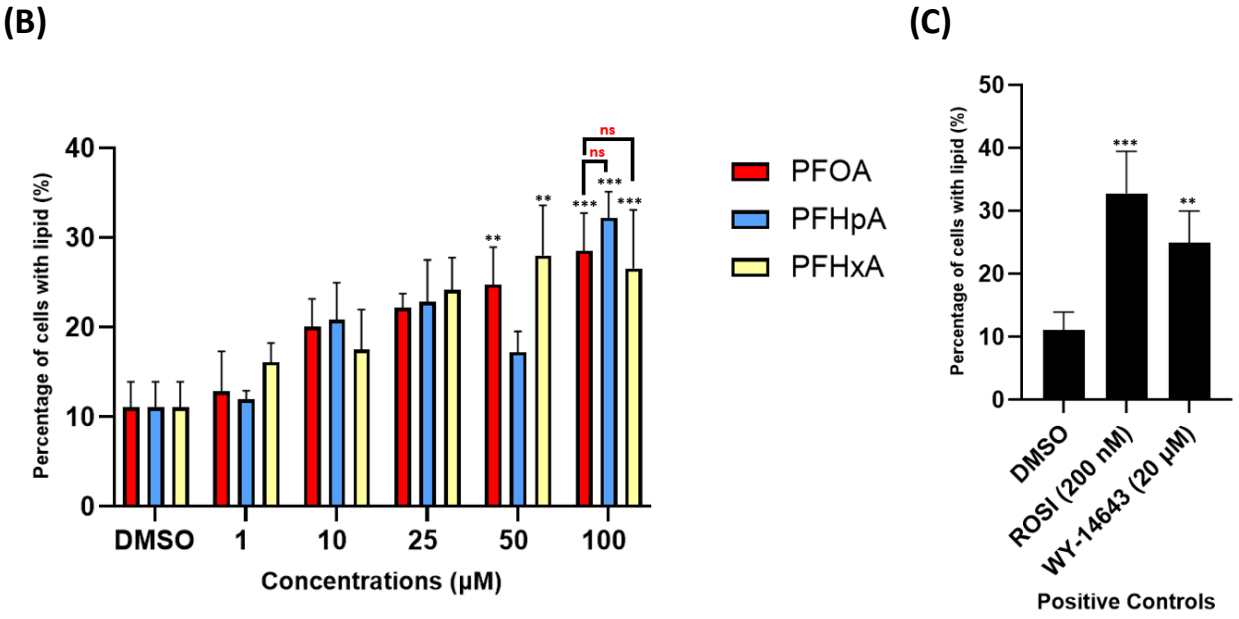

Figure 5. Visualization of lipid accumulation and lipid quantification of 3T3-L1 preadipocytes treated with PFOA, PFHpA or PFHxA from concentrations ranging between 0-100 µM. 3T3-L1 preadipocytes were induced to differentiate in 96-well plates for 8 days in the presence of 500 µM IBMX (day 0-2), 100 nM insulin (day 0-8) and PFOA, PFHpA or PFHxA (0-100 µM). Positive controls were treatments with 200 nM ROSI (day 0-2) or 20 µM WY-14643 (day 0-8). Lipid accumulation was (A) visualized using BODIPY staining and (B) lipids were quantified. Lipid accumulation was normalized to DAPI staining and expressed as fold over DMSO control. Data was represented the mean fold change ± standard error of mean (SEM) where *P<0.05, **P<0.01, ***P<0.001 relative to vehicle control, and ns (non-significant), *P<0.05, **P<0.01, ***P<0.001 relative to PFOA-treated cells, using a two-way ANOVA or one-way ANOVA followed by Tukey's multiple comparisons test or Dunnett's multiple comparisons test, respectively.

3.4 Activation of nuclear receptors (PPARγ and PPARα) in the presence of PFCAs (PFOA, PFHpA and PFHxA)

As we have established in our study that PFCA treatments induced adipogenesis, we sought to uncover the mechanism by which adipogenesis is occurring upon PFCA treatments. The activation of PPARs is critical for various physiological processes, such as metabolism, inflammation, and adipocyte differentiation (Christofides *et al.,* 2021). PPARγ activation by ROSI and PPARα activation by WY-14643 have been previous established to promote adipogenesis (Brun *et al.*, 1996). Interestingly, PFAS have been associated with the activation of PPARs. Previous research has demonstrated that PFOA-treated cells induce adipogenesis through PPARγ activation (Yamamoto *et al.,* 2015). Studies have also shown that PFOA and PFHxA were able to activate PPARα (Lefebvre *et al.,* 2006). However, the activation of both PPAR receptors upon PFHpA treatments have not been previously investigated, so to evaluate the activation of PPARγ and PPARα by PFCAs, human PPARγ and PPARα transactivation assays were performed. The activation of human PPARγ and PPARα were assessed in the presence of PFOA, PFHpA or PFHxA at concentrations ranging from 0-100 µM.

3.4.1 *PFOA, but not PFHpA and PFHxA increase PPARγ transcriptional activity*

To assess if these PFCAs are activating the transcription of PPARγ, I performed a PPARγ transactivation assay in the presence of PFOA, PFHpA and PFHxA ranging from 0-100 µM. Among the three PFCAs examined, both PFOA and PFHpA increased PPARγ transcriptional activity as shown by increased luciferase levels in the reporter assay, relative to control (Figure 6A). Specifically, at 100 µM, PFOA demonstrated substantial activity, showing a 4.1-fold

increase in PPARγ activity, relative to the solvent control. PFOA did not show significant PPARγ activity at lower concentrations (0-50 µM). Conversely, PFHpA and PFHxA did not induce any discernible effect on PPARγ activity. The PPARγ agonist, ROSI, used as a positive control, demonstrated increasing dose response, confirming the validity of the transactivation assay (Figure 6B).

3.4.2 *PFOA, PFHpA and PFHxA increase PPARα transcriptional activity*

In order to assess if these PFCAs are also activating the transcription of PPARα, I performed a PPARα transactivation assay in the presence of PFOA, PFHpA and PFHxA ranging from 0-100 µM. All three PFCAs increased the transcriptional activity of PPARα compared to the DMSO control (Figure 6C). Specifically, PFOA at 100 µM demonstrated a substantial 16.0-fold increase in PPARα activation relative to the solvent control, with significant activation observed even at concentrations as low as 25 µM (2.3-fold increase relative to control), but below this concentration (0-10 µM), no significant PPARα activation was seen. Similarly, PFHpA at 100 µM showed a notable 9.3-fold increase in PPARα transcriptional activity, relative to the solvent control, with significant activation detected at concentrations as low as 25 µM (1.9-fold increase relative to control), but below this concentration (0-10 µM), no significant PPARα activation was seen. PFHxA at 100 µM displayed a moderate 2.4-fold increase in PPARα activation relative to the solvent control, but below this concentration (0-50 µM), no significant PPARα activation was seen. The positive control, GW7647, demonstrated significant activation of PPARα, in an increasing dose-response, confirming the validity of the transactivation assay (Figure 6D).

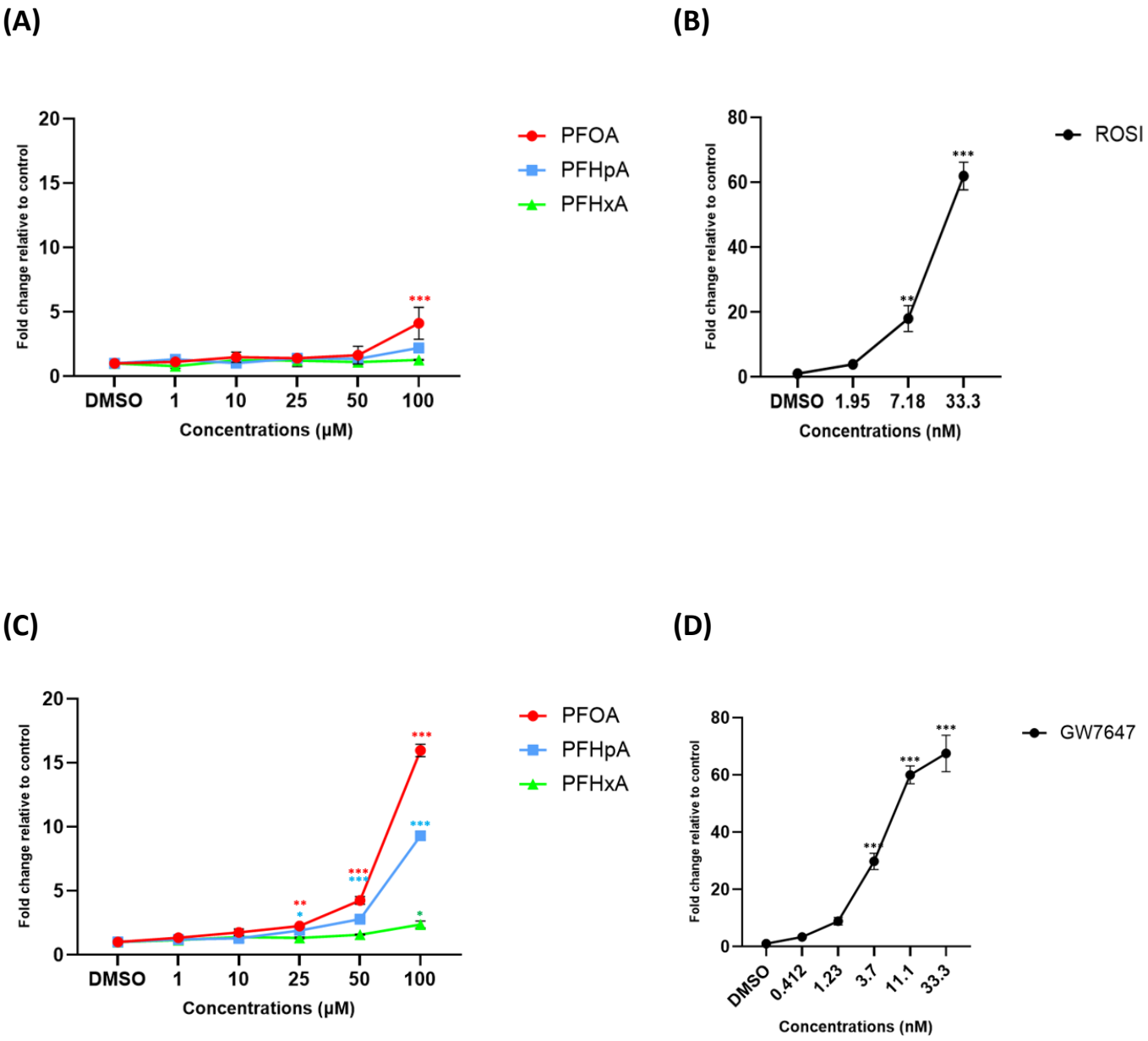

Figure 6. Nuclear receptor activation analysis of PFOA, PFHpA or PFHxA from concentrations ranging between 0-100 µM. Human PPARγ and PPARα reporter assay systems (Indigo Biosciences) were used to quantify (A) PPARγ and (B) PPARα transcriptional activity, respectively. Positive controls were ROSI (PPARγ agonist) or GW7647 (PPARα agonist). The solvent control used was DMSO. Data was represented by the mean fold change ± standard error of mean (SEM) where *P<0.05, **P<0.01, ***P<0.001 relative to vehicle control, using a two-way ANOVA followed by Tukey's multiple comparisons test.

3.5 Transcriptional expression analysis of genes involved in fatty acid oxidation in the presence of PFOA, PFHpA or PFHxA

Although PPARα activation does play a role in inducing adipogenesis, PPARα is well known for its function in inducing fatty acid oxidation (Brun *et al.,* 1996; Lefebvre *et al.*, 2006). A Tsuyoshi Goto study demonstrated the upregulation of genes involved in fatty acid oxidation, specifically *ACOX1*, *UCP3* and *CPT1b*, in 3T3-L1 preadipocytes treated with a PPARα agonist, GW7647 (Tsuyoshi Goto *et al.,* 2011). Previously in our study, we demonstrated that the transcriptional activity of PPARα increased upon PFCA treatments, prompting us to look deeper into the involvement of PFCA exposure with fatty acid oxidation. In PFCA-treated 3T3-L1 cells, we examined the expression of three genes involved in fatty acid oxidation were analyzed: *ACOX1*, *UCP3*, and *CPT1b*.

3.5.1 *PFCA treatments did not affect the mRNA levels of ACOX1 in 3T3-L1 preadipocytes*

In order to assess if other PFAS induce fatty acid oxidation, we looked at the expression of *ACOX1* in PFAS-treated cells. No significant expression changes were observed in *ACOX1* with any of the PFCA treatments (Figure 7A). However, cells treated with the positive control, WY-14643 at 20 μM, showed notable increases of 3.0-fold, relative to the solvent control (Figure 6B). Cells treated with ROSI at 200 nM demonstrated a 5.9-fold increase in *ACOX1* expression relative to control (Appendix - Supplemental Figure 2A).

3.5.2 *PFOA-treated cells up-regulate the mRNA levels of UCP3 in 3T3-L1 preadipocytes*

To assess if other PFAS are involved in promoting fatty acid oxidation, we looked at the expression of *UCP3* in PFAS-treated cells. PFOA-treated cells significantly expressed of *UCP3* in 3T3-L1 preadipocytes, relative to control (Figure 7C). Specifically, PFOA-treated cells at concentrations of 50 µM and 100 µM demonstrated 3.0-fold and 5.1-fold increases in *UCP3* expression relative to the solvent control, respectively. PFOA-treated cells did not demonstrate any significant *UCP3* expression at lower concentrations (0-25 µM). PFHpA and PFHxA-treated cells did not induce any significant change in *UCP3* expression. Significant changes in *UCP3* expression were seen between the PFOA-treated cells and PFHpA-treated cells. Significant changes in *UCP3* expression were also seen between PFOA-treated cells and PFHxA-treated cells. Cells treated with the positive control, WY-14643 at 20 µM a showed an increase of 10.4-fold, relative to the solvent control (Figure 7D). Cells treated with ROSI at 200 nM demonstrated a 59.3-fold increase in *UCP3* expression relative to control (Appendix - Supplemental Figure 2B).

3.5.3 *PFHpA-treated cells up-regulate the mRNA levels of CPT1b in 3T3-L1 preadipocytes*

In order to determine if other PFAS induce fatty acid oxidation, we looked at the expression of *CPT1b* in PFAS-treated cells. Among the three PFCAs tested, only PFHpA-treated cells exhibited significant expression of *CPT1b* (Figure 7E). Specifically, PFHpA-treated cells at 100 µM demonstrated a 2.3-fold increase in *CPT1b* expression relative to the solvent control. PFHpA-treated cells did not demonstrate significant *CPT1b* expression at lower concentrations (0-50 µM). PFOA and PFHxA-treated cells did not induce any significant change in *CPT1b*

expression. Cells treated with the positive control, WY-14643 at 20 µM, showed notable increases of 4.6-fold, respectively, relative to the solvent control (Figure 7F). Cells treated with ROSI at 200 nM demonstrated a 5.3-fold increase in *CPT1b* expression relative to control (Appendix - Supplemental Figure 2C).

(A)

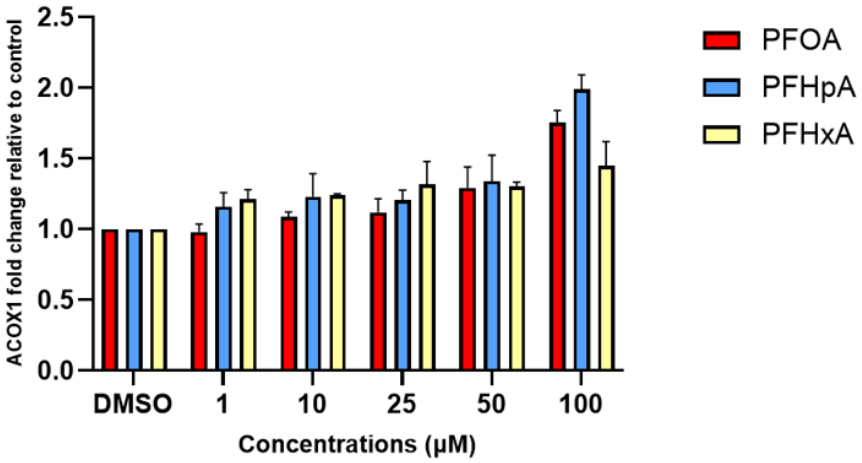
ACOX1 fold change relative to control
2.5
2.0
1.5
1.0
0.5
0.0
DMSO
1
10
25
50
100
Concentrations (μM)
PFOA
PFHpA
PFHxA

(B)

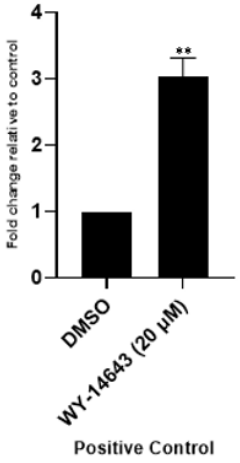
Fold change relative to control
4
3
2
1
0
**
DMSO
WY-14643 (20 μM)
Positive Control

(C)

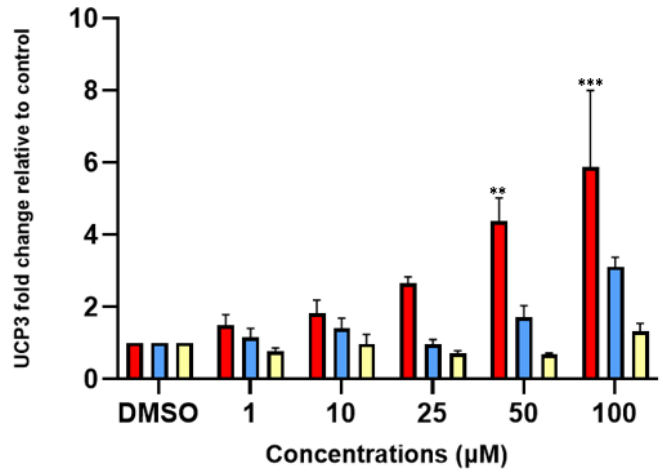
UCP3 fold change relative to control
10
8
6
4
2
0
**
***
DMSO
1
10
25
50
100
Concentrations (μM)
PFOA
PFHpA
PFHxA

(D)

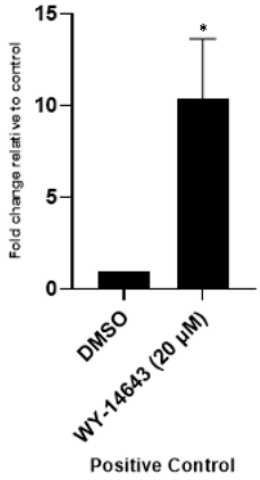
Fold change relative to control
15
10
5
0
*
DMSO
WY-14643 (20 μM)
Positive Control

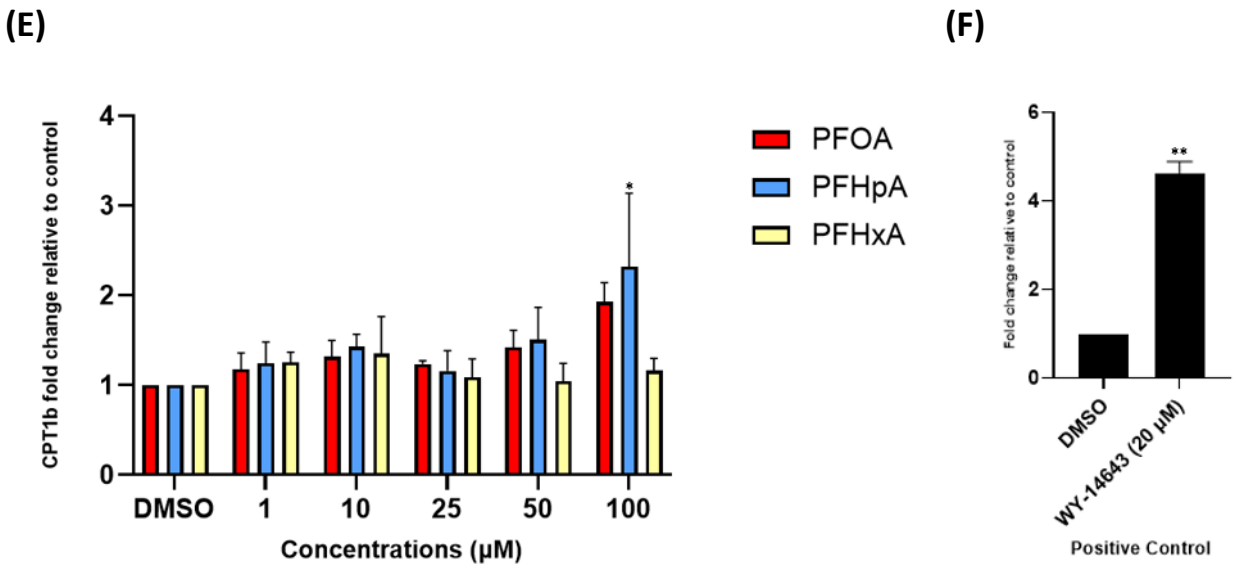

Figure 7. Transcriptional expression analysis of genes involved in fatty acid oxidation of 3T3-L1 preadipocytes treated with PFOA, PFHpA and PFHxA from concentrations ranging between 0-100 µM. 3T3-L1 preadipocytes were induced to differentiate in 6-well plates for 6 days in the presence of 500 µM IBMX (day 0-2), 100 nM insulin (day 0-6) and one of the three test PFAS chemicals (0-100 µM). Positive controls were treatments with 20 µM WY-14643. The solvent control used was DMSO. On day 6, cells were harvested, and RNA was isolated. qPCR analysis was used to assess the expression levels of three lipolysis genes: (A) *ACOX1*, (B) *UCP3*, and (C) *CPT1b*. Levels were normalized to *β-actin* levels and expressed as fold over solvent control. Data was represented the mean fold change ± standard error of mean (SEM) where *P<0.05, **P<0.01, ***P<0.001 relative to vehicle control, using a two-way ANOVA or one-way ANOVA followed by Tukey's multiple comparisons test or Dunnett's multiple comparisons test, respectively.

3.6 Differentiating PPARγ-induced adipogenesis and PPARα-induced adipogenesis using PCR array analysis

From our previous results, we demonstrated that adipogenesis occurs upon PFCA treatment. Next, we looked at the expression of genes involved in adipogenesis upon low and high concentrations, mainly to focus on the phenotype of the adipocytes formed from PFCA treatments. To achieve this, we used PCR Array kits with genes specific to mouse adipogenesis and the maintenance of mature adipocytes. We also aimed to differentiate between PPARγ-induced adipogenesis and PPARα-induced adipogenesis. We aimed to identify genes that are specifically induced by ROSI treatment and those that are specifically induced by WY-14643 treatment.

3.6.1 *Insignificant transcript expression analysis following PFCA treatment at low and high concentrations*

Transcript expression was analyzed following low and high concentrations of PFOA-treated cells (10 and 100 µM), PFHpA-treated cells (25 and 100 µM) and PFHxA-treated cells (25 and 100 µM). Upregulation was observed in key genes involved in lipid and glucose metabolism (Figure 8A). However, for the majority of these genes upon all treatments, the p-values were insignificant ($p > 0.05$), as seen in the volcano plots (Figure 8D-I, Appendix – Table 3).

3.6.2 *PPARγ-induced adipogenesis and PPARα-induced adipogenesis express the same genes in this PCR Array*

The PCR array results demonstrated that the ROSI and WY-14643 treatments upregulated the same genes significantly, with the ROSI treatment consistently inducing higher expression levels than WY-14643 treatments. For instance, both treatments significantly increased the expression of three adipokines: adiponectin (Adipoq), adipsin (Cfd), and leptin (Lep), depicted in the heat map and volcano plots (Figure 8A-C, Appendix – Table 2). Specifically, the ROSI treatment led to a 26.71-fold increase in Adipoq expression, compared to an 11.16-fold increase with the WY-14643 treatment. For Cfd, ROSI induced a 37.36-fold increase, while WY-14643 treatments induced a 9.57-fold increase. Lep expression was increased by 16.98-fold with the ROSI treatment and by 4.52-fold with WY-14643 treatments.

(A)

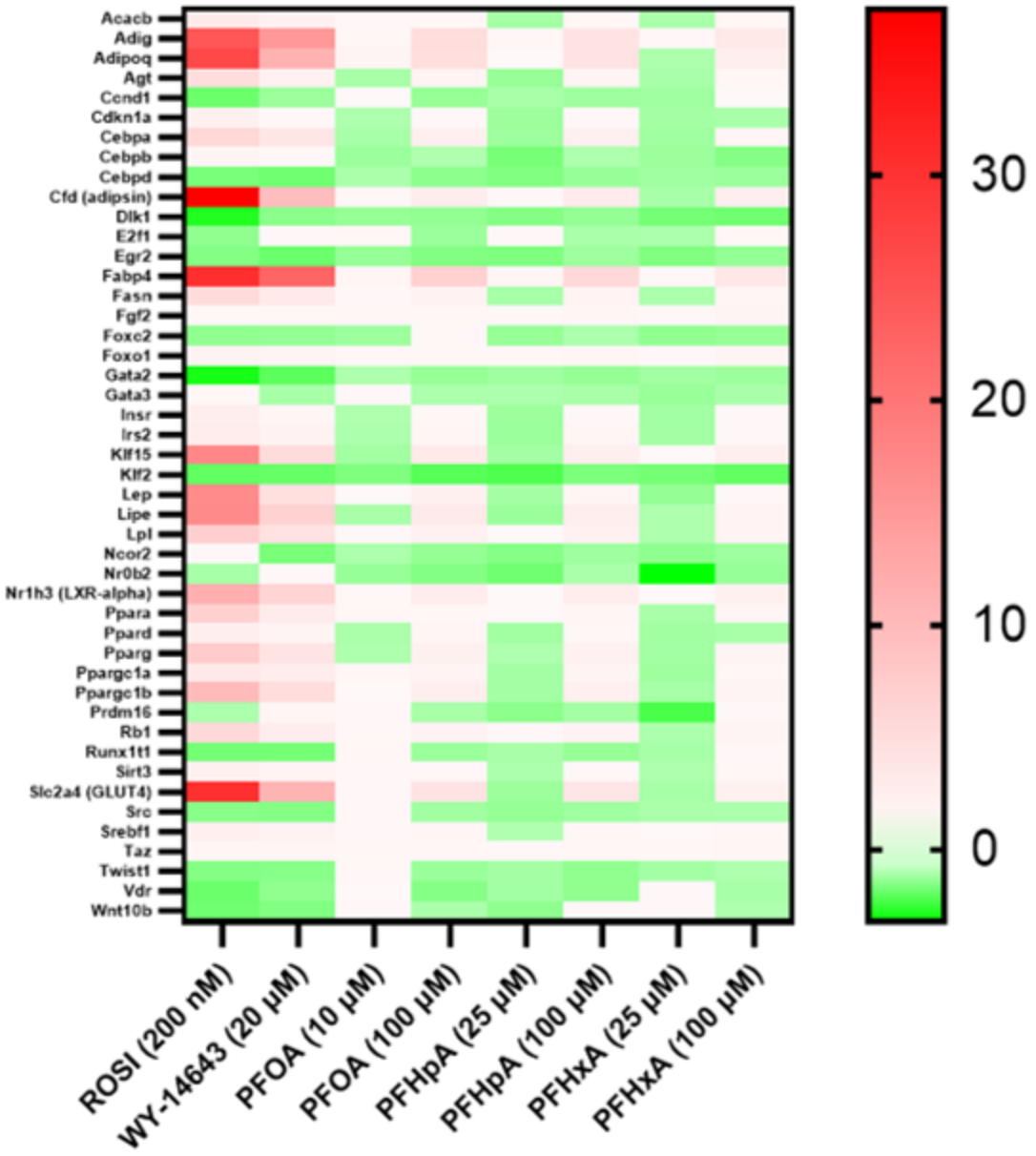
Acacb
Adig
Adipoq
Agt
Ccnd1
Cdkn1a
Cebpa
Cebpb
Cebpd
Cfd (adipsin)
Dlk1
E2f1
Egr2
Fabp4
Fasn
Fgf2
Foxc2
Foxo1
Gata2
Gata3
Insr
Irs2
Klf15
Klf2
Lep
Lipe
Lpl
Ncor2
Nr0b2
Nr1h3 (LXR-alpha)
Ppara
Ppard
Pparg
Ppargc1a
Ppargc1b
Prdm16
Rb1
Runx1t1
Sirt3
Slc2a4 (GLUT4)
Src
Srebf1
Taz
Twist1
Vdr
Wnt10b
30
20
10
0
ROSI (200 nM)
WY-14643 (20 µM)
PFOA (10 µM)
PFOA (100 µM)
PFHpA (25 µM)
PFHpA (100 µM)
PFHxA (25 µM)
PFHxA (100 µM)

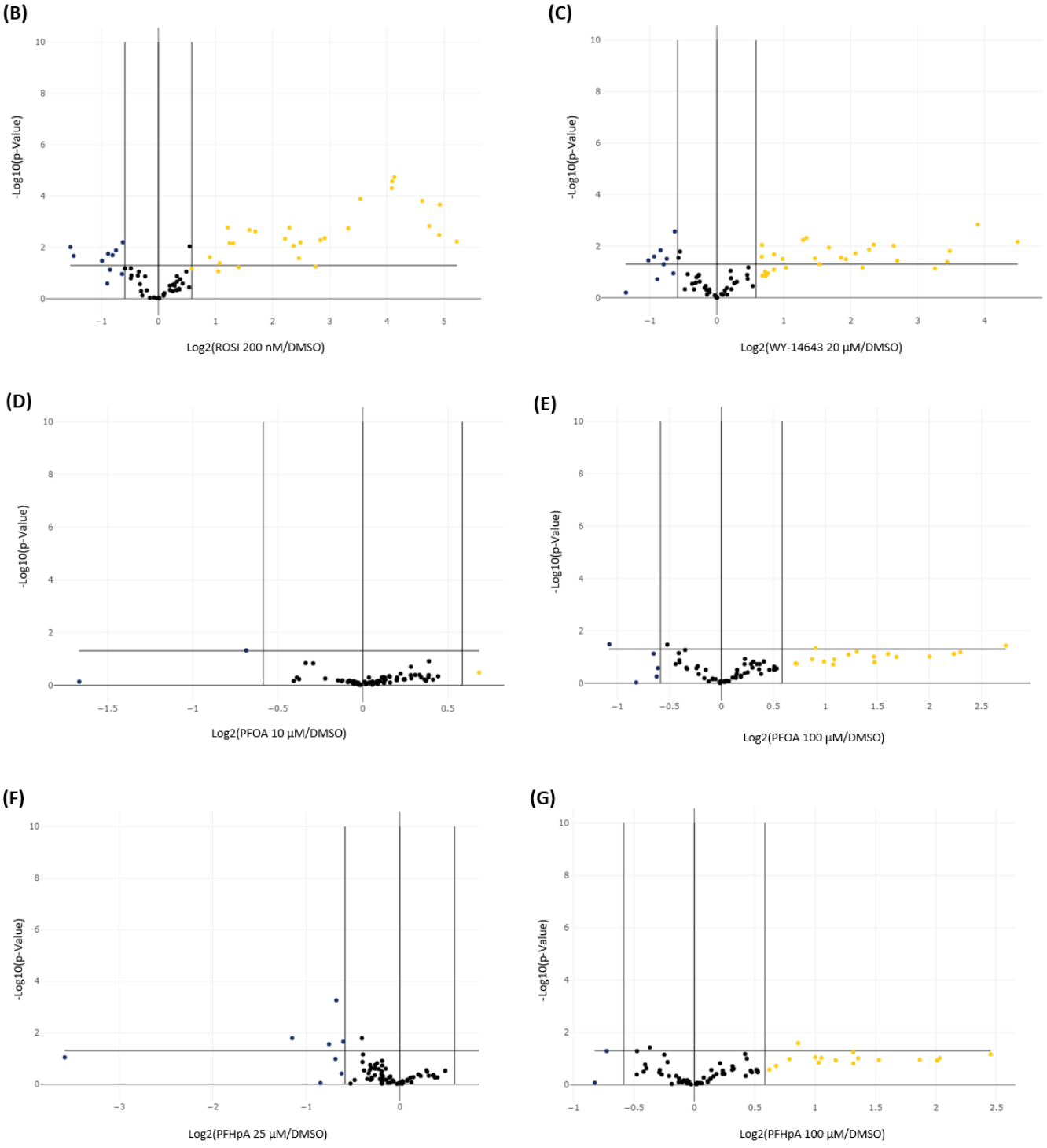
(B)
-Log10(p-Value)
Log2(ROSI 200 nM/DMSO)
(C)
-Log10(p-Value)
Log2(WY-14643 20 µM/DMSO)
(D)
-Log10(p-Value)
Log2(PFOA 10 µM/DMSO)
(E)
-Log10(p-Value)
Log2(PFOA 100 µM/DMSO)
(F)
-Log10(p-Value)
Log2(PFHpA 25 µM/DMSO)
(G)
-Log10(p-Value)
Log2(PFHpA 100 µM/DMSO)

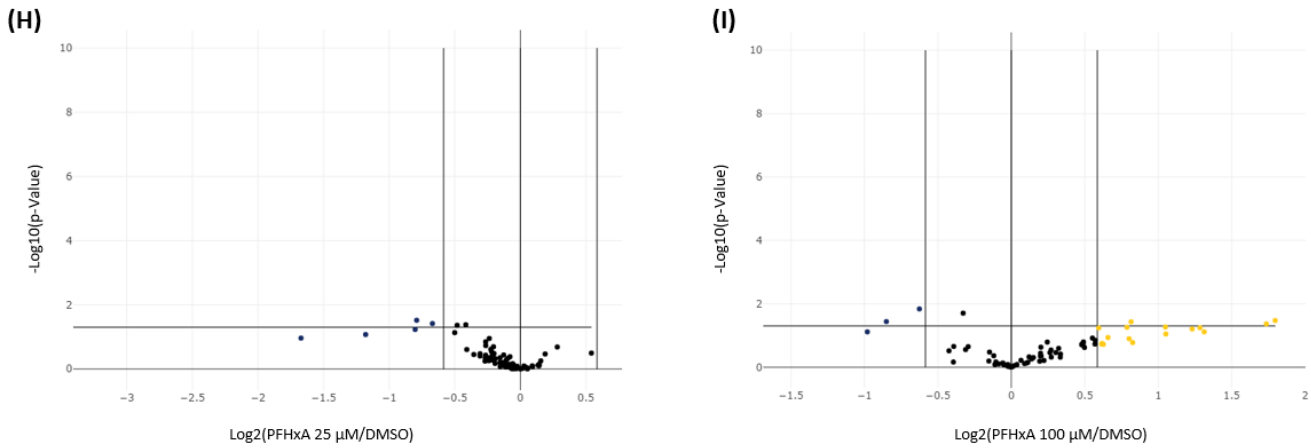

Figure 8. Transcriptional expression analysis of multiple genes involved in adipocyte differentiation and the maintenance of the mature adipocyte of 3T3-L1 preadipocytes treated with PFOA, PFHpA and PFHxA from concentrations ranging between 0-100 µM. Mouse adipogenesis RT^2 Profiler PCR Array kit from Qiagen were used to analyze the expression of major genes involved in white and brown adipose tissue adipogenesis, and adipocyte maintenance, such as hormones, adipokines, enzymes and transcription factors. cDNA was synthesized using the RT^2 First Strand Kit, and genomic DNA was eliminated. Real-time PCR reactions were performed using CFX96 Real-Time System C1000 Thermal Cycler at the recommended cycling conditions. Levels were normalized to β-*actin* levels and expressed as fold over solvent control. (A) A heatmap representing relative transcriptional expression of genes involved in adipogenesis and the maintenance of the mature adipocyte in alphabetical order. The red-green gradient represents fold regulation of the genes relative to the solvent control, red representing upregulation and green representing downregulation. Heatmap was generated using GraphPad Prism. Volcano plot showing the separation of differentially expressed genes from adjusted p-value and log fold change for each individual treatment: (B) ROSI 200 nM, (C) WY-14643 20 µM, (D) PFOA 10 µM, (E) PFOA 100 µM (F) PFHpA 25 µM, (G) PFHpA 100 µM, (H) PFHxA 25 µM, and (I) PFHxA 100 µM. The x-axis represents the log base 2 of the fold change value of each gene relative to DMSO control. The y-axis represents the negative log base 10 of the adjusted p-value of differentially expressed genes. Volcano plot was generated by GeneGlobe.

4.0 DISCUSSION

PFAS are human-made chemicals found in many everyday-use items, because of their water-resistant properties (Hall *et al.* 2020). Due to their strong chemical properties, these chemicals are very persistent in the environment. The underlying issue with this is that PFAS exposure has demonstrated to cause a wide range of adverse health effects, such as having implications with NAFLD, hypothyroidism and reproduction, just to name a few (Wang et al., 2013; Melzer et al., 2010; Šabović et al., 2020). Previous research has shown that PFAS have the potential to be obesogens. PFOA has been shown to promote adipogenesis in 3T3-L1 preadipocytes (Yamamoto et al., 2015). PFOA and other longer-chained PFCAs are banned in Canada, which has promoted the use of shorter-chained PFCAs as substitutes to longer-chained PFCAs (i.e. PFHpA and PFHxA) (Legislative Services Branch, 2024). This is concerning as the health implications of these shorter-chained PFCAs require further investigation. Therefore, in this study, we wanted to uncover the potential impacts of shorter-chained PFCAs (PFHpA and PFHxA) on adipogenesis and determine the mechanisms through which these PFCAs may induce adipogenesis.

The first aim of this study was to test the cell viability of three PFCAs on 3T3-L1 preadipocytes. Cell viability was tested using an Alamar Blue assay. This assay looks at cell viability by monitoring the reducing environment of a living cell through REDOX reactions. As Alamar Blue enters the cytoplasm, it is converted to its reduced form by mitochondrial enzyme activity, suggesting that Alamar Blue reduction may signify impairment in cellular metabolism (Al-Nasiry *et al.*, 2007; Rampersad, 2012). Since this assay can detect impairment in cellular metabolism, the cytotoxicity of PFOA, PFHxA and PFHpA can be measured at varying concentrations to determine which concentrations are toxic to the cell line used. This assay aided

this study in establishing which concentrations to expose cells with when looking at adipogenic differentiation in 3T3-L1 preadipocytes. The concentrations of PFOA, PFHpA and PFHxA tested in the Alamar Blue assay ranged from 0-100 μM. Alamar blue assay results demonstrated that none of the chemicals were toxic to the 3T3-L1 preadipocyte cell line (Figure 3). These results validated the use of the tested concentrations for further investigation into adipogenesis under PFCA exposure.

Adipocyte differentiation can be confirmed through various methods, one being assessing the expression of adipogenic markers. Studies have demonstrated PFOA-treated cells in 3T3-L1 preadipocytes to significantly upregulate *FABP4* and *LPL* in 3T3-L1 preadipocytes (Ma *et al.,* 2018). Although there are no studies looking at *perilipin 1* expression in 3T3-L1 cells upon PFOA-treated cells, the expression of *perilipin 2* has been shown to be upregulated upon PFOA-treatment in primary human hepatocytes at 10 μM (Beggs *et al.*, 2016). Our study is the first to look at transcriptional expression of *FABP4*, *LPL* and *perilipin* upon PFHpA and PFHxA treatment. In our study, PFOA-treated cells were able to significantly express *FABP4* at 100 μM (Figure 4A), *LPL* at 100 μM (Figure 4C) and *perilipin* at 50 μM and 100 μM (Figure 4E). PFHpA-treated cells were able to significantly express *FABP4* at 100 μM, *LPL* at 100 μM and *perilipin* at 100 μM. PFHxA-treated cells were able to significantly express *LPL* at 100 μM and *perilipin* at 100 μM. The high expression of these genes indicates potential adipogenesis, yet additional verification was required for conclusive evidence.

When comparing the expression levels of the adipogenic markers between the different chemical treatments, the expression of both *FABP4* and *perilipin* in the PFOA-treated cells were significantly increased relative to the expression seen in PFHxA-treated cells, but no significant changes in *FABP4* and *perilipin* expression were seen between PFOA-treated cells and PFHpA-

treated cells. This means that although PFHxA is able to induce adipogenesis, it is to a lesser extent compared to PFOA-induced adipogenesis. Whereas for PFOA and PFHpA, the expression levels of these adipogenic markers were similar between one another. The similarity between a substance that is banned in Canada (PFOA) and a substance that remains legal in Canada (PFHpA), is quite concerning. Given the negative health implications of PFOA, specifically its association with metabolic syndrome, PFHpA has the potential risk of producing similar effects.

To further confirm that adipogenesis was present upon PFCA treatments, lipid accumulation within 3T3-L1 adipocytes were quantified, using high-throughput imaging. High-throughput imaging involves employing automated microscopy and image analysis to visualize and quantitatively capture cellular characteristics (Pegoraro & Misteli, 2017). In previous studies, PFOA-treated 3T3-L1 cells have shown significant lipid accumulation at 100 μg/mL and 100 μM (Ma *et al.*, 2018; Yamamoto *et al.*, 2015). No studies have looked at lipid accumulation from PFHpA and PFHxA-treated cells. By staining 3T3-L1 adipocytes with DAPI to identify individual cell nuclei and BODIPY staining identify lipids within adipocytes, percentage of cells containing lipid can be quantified relative to number of cells present (Tarnowski *et al.*, 1991; Spangenburg *et al.*, 2011). On day 8 of differentiation, percentage of 3T3-L1 adipocytes containing lipid were quantified. Lipid quantification results demonstrated increased lipid accumulation upon PFCA-treated cells at higher concentrations (Figure 5B). PFOA-treated cells were able to significantly increase lipid accumulation at 50 μM and 100 μM, PFHpA-treated cells were able to significantly increase lipid accumulation at 50 μM and 100 μM, and PFHxA-treated cells were able to significantly increase lipid accumulation at 100 μM.

The upregulation of *FABP4* seen in this study potentially demonstrate an enhanced capacity of fatty acid transport within the cells. This is consistent with the increased lipid

accumulation, as FABP4 is required to traffic fatty acids to lipid droplets for storage. The upregulation of *LPL* seen in our results possibly show increased fatty acid uptake and lipid storage, which is consistent with the increased lipid accumulation seen within our cells. The *perilipin* upregulation potentially demonstrates increased lipid droplet protection of lipid droplets. This also aligns with the increased lipid accumulation seen within our 3T3-L1 cells.

When comparing the lipid accumulation between the different chemical treatments, there were no significant differences in the lipid accumulation when comparing the PFOA-treated cells to the PFHpA-treated cells and the PFOA-treated cells to the PFHxA-treated cells. This means that in 3T3-L1 preadipocytes, PFOA treatments did not have much change in lipid accumulation compared to the treatments of its substitutes, PFHpA and PFHxA.

The activation of PPARγ and PPARα are proven to induce and drive the process of adipogenesis, culminating in the differentiation and maturation of adipocytes (Brun *et al.,* 1996; Yamamoto *et al.,* 2015). These nuclear receptors are activated by endogenous ligands, such as fatty acids and their derivatives. For PPARγ activation, literature claims that it is activated by PFOA at high concentrations, and PFHxA does not activate PPARγ at high concentrations (Yamamoto *et al.,* 2015; Evans *et al.,* 2022). No previous studies have looked at PPARγ activity in response to PFHpA treatment. The findings of this study demonstrated that PFOA was able to significantly activate PPARγ, but not PFHpA and PFHxA (Figure 6A). For PPARα activation, the literature claims that it is significantly activated by PFOA and PFHxA at concentrations as low as 50 μM (Behr *et al.,* 2020). No studies have investigated PPARα activity in response to PFHpA treatment. Our results demonstrated that PFOA, PFHpA and PFHxA significantly activate PPARα (Figure 6C). This is most-likely due to the structural similarity between PFAS chemicals and fatty acids (Roth *et al.,* 2020). Additionally, the hydrophobic tendencies of these

PFCAs may enable them to interact with the hydrophobic pockets within the ligand-binding domain of the PPAR receptors (Almeida *et al.,* 2021).

The findings indicate that PFHpA and PFHxA notably activated PPARα but not PPARγ. Despite this, examination of transcriptional expression and lipid accumulation demonstrated their capacity to induce adipogenesis. Given that activation of PPARγ and PPARα are able to promote adipogenesis, the fact that both PFHpA and PFHxA exclusively activated PPARα suggests they induce adipogenesis through PPARα activation.

PPARα activation is also associated with fatty acid oxidation. This led to investigating the expression of genes involved in fatty acid oxidation, specifically *ACOX1, UCP3, and CPT1b*. In previous studies, PFOA-treated 3T3-L1 cells have demonstrated significant expression of *ACOX1* in at higher concentrations, and PFOA-treated cells at high concentrations increased *CPT1b* expression in zebrafish (Watkins *et al.*, 2015; Sun *et al.,* 2023). No studies have looked at *UCP3* expression in cells upon PFOA-treatments. PFHpA-treated cells in human hepatocytes have shown significant upregulation in *ACOX1* expression (David *et al.,* 2023). No previous studies have looked at *UCP3* and *CPT1b* expression in cells upon PFHpA-treatments. No prior studies have looked at *ACOX1*, *UCP3* and *CPT1b* expression in cells upon PFHxA-treatments. In this study, *ACOX1* was not significantly expressed by PFOA, PFHpA or PFHxA treatments (Figure 7A). *UCP3* was significantly expressed by PFOA treatments at 50 μM and 100 μM (Figure 7C). The upregulation of *UCP3* demonstrate enhanced export of fatty acids from the mitochondria to the cytoplasm, preventing fatty acid accumulation inside the mitochondrial matrix (Schrauwen *et al.,* 2001c). *CPT1b* was significantly expressed by PFHpA at 100 μM (Figure 7E). *CPT1b* upregulation show increased transport of long-chained fatty acids into the mitochondria to undergo fatty acid oxidation (McGarry & Brown, 1997). Overall, these results

indicate that different PFAS compounds may have distinct effects on the expression of genes involved in fatty acid oxidation.

Interestingly, in the transcriptional expression analysis of the positive control treatments, the PPARγ agonist, ROSI, induced higher expression of all three fatty acid oxidation genes compared to the PPARα agonist, WY-14643. This outcome was unexpected, as it was initially hypothesized that WY-14643 treatments, known to activate PPARα, would lead to greater induction of fatty acid oxidation genes than the ROSI treatment, which is involved in PPARγ activation. Research has shown ROSI treatments in mice to downregulate *UCP3* and *CPT1b* expression and no effect on *ACOX1* expression (Chang *et al.,* 2014). Moreover, previous studies have indicated that PPARγ activation may decrease intracellular concentrations of carnitine and reduce labeling of tricarboxylic acid (TCA) cycle intermediates and shorter-chained fatty acids from U-13C palmitate, suggesting that PPARγ activation could potentially lead to a reduction in fatty acid oxidation (Roberts *et al.*, 2011). WY-14643 treatments have demonstrated the upregulation of *ACOX1, UCP3* and *CPT1b* in *in* vivo models (Yang *et al.,* 2022; Song *et al.,* 2016; Brocker *et al.,* 2017). However, contrary to these studies, our findings suggest that ROSI (PPARγ agonist) treatments resulted in more pronounced upregulation of fatty acid oxidation genes, in comparison to WY-14643 (PPARα agonist) treatments (Figure 7, Supplemental Figure 2). Moreover, no subsequent non-specific activation of PPARα was seen from ROSI treatments, and no non-specific activation of PPARγ was seen by WY-14643 treatments (Appendix – Supplemental Figure 1).

Based on these findings, we postulate that the genes *ACOX1, UCP3,* and *CPT1b* may not be exclusively associated with fatty acid oxidation, and their regulation by PPARα and PPARγ agonists may involve additional or alternative metabolic pathways beyond fatty acid oxidation.

Further investigation is warranted to elucidate the complex mechanisms underlying the regulation of these genes by PPAR agonists and their role in cellular metabolism.

The observation that *ACOX1, UCP3*, and *CPT1b* were not exclusively associated with fatty acid oxidation prompted us to question whether there are specific genes that are regulated upon specific PFCA treatments. Since these compounds were able to induce adipogenesis, we asked whether the resulting adipocyte would have the same phenotype as ROSI-treated adipocytes. PCR arrays are available in pre-designed panels targeting specific gene sets or biological pathways. These focused gene panels enable targeted analysis of genes relevant to particular research interests or biological processes. Our interest in the phenotype of the adipocytes upon PFCA treatments, led us to utilize a PCR array which examines the expression of 84 different genes involved in adipogenesis and the maintenance of the mature adipocyte. While the high concentration treatments did lead to elevated expression levels in genes similar to those observed in positive control treatments, the statistical significance of these findings were insufficient to draw any conclusive statements ($p > 0.05$) (Figure 8A, 8D-I).

Although no significant data was shown when trying to assess the phenotypes of adipocytes upon PFCA treatment, using these PCR arrays we could possibly distinguish between adipogenesis induced by PPARγ activation and that induced by PPARα activation. This realization marked a significant breakthrough, suggesting a promising avenue for further investigation into the distinct molecular signatures associated with PPARγ- and PPARα-mediated adipogenesis using targeted transcriptional expression analysis. This can also create an avenue to confirm which mechanism PFHpA-treated adipocytes and PFHxA-treated adipocytes go through to induce adipogenesis.

In our investigation into adipogenesis, we utilized mouse adipogenesis PCR arrays to examine the transcriptional expression patterns influenced by PPARγ and PPARα during adipogenesis. Specifically, we focused on comparing the effects of ROSI and WY-14643 treatments, aiming to identify any differences in transcriptional expression that might indicate distinct pathways of adipogenesis mediated by these receptors. The two treatments significantly upregulated the same genes, with ROSI consistently eliciting higher expression levels compared to WY-14643 (Figure 8A, 8B-C). However, because treatments conditions with ROSI (cells treated for 2-days) and WY-14643 (cells treated for 6-days) were different, no conclusions can be made.

5.0 LIMITATIONS

The results of this study clearly demonstrated that PFOA, PFHpA, and PFHxA were evaluated at concentrations ranging from 0 to 100 μM. A 2003 study reported human serum concentrations of PFOA in the United States as high as 0.1 μM (Olsen *et al.*, 2003). Given that concentrations of up to 100 μM of PFCAs in humans are exceedingly rare, using such high concentrations in our study may be physiologically irrelevant.

Research has shown that PFAS adsorb to plastic surfaces with high affinity, with PFCAs exhibiting adsorption rates of up to 21% (Llorca *et al.*, 2018). PFCAs also display a higher tendency to adsorb to plastics compared to PFSAs and perfluoroalkyl sulphonamides (FASAs). This raised a concern because all the pipette tips, microcentrifuge tubes, test tubes, and culture plates utilized in this study, which came into contact with PFCAs, were made of plastic. Due to

the strong affinity of PFCAs for plastic, a significant portion of the chemicals may adhere to these plastic surfaces, resulting in less of the chemical entering the cells.

To address the issue of PFCA adsorption to plastic culture dishes and ensure more accurate measurements of PFCA concentrations entering the cells, several mitigation strategies can possibly be implemented. Replacing plastic culture plates with glass culture plates could potentially reduce PFCA adsorption to the culture plate surface. Glass surfaces are primarily composed of silica (SiO_2) and lack the organic functional groups that can interact with the C-F bonds of PFCAs (Azizi *et al.,* 2021; Hellsing *et al.,* 2016). In contrast, plastic surfaces often contain carbon and hydrogen in their polymer chains, which facilitate the adsorption of PFCAs. However, some studies advise against using glass surfaces, claiming that glass adsorbs PFAS analytes and that PFAS samples should not come into contact with glass containers (Hansen *et al.,* 2002; BSI, 2009). Silica-coated plates have also been used in *in vitro* models and could potentially mitigate PFAS adsorption (Taub *et al.,* 1998). These methods are preventative measures aimed at increasing the amount of PFCA that enters cells, but the exact concentration of PFCA entering the cells remains in question. Using analytical techniques such as liquid chromatography-mass spectrometry (LC-MS/MS), we can isolate, identify, and quantify the exact concentrations of PFCAs that have entered 3T3-L1 cells (Roberts *et al.,* 2019). LC-MS/MS provides a high level of sensitivity and specificity, enabling precise measurement of PFCA levels within the cellular environment. Additionally, enzyme-linked immunosorbent assay (ELISA) tests, which employ antibodies designed to specifically bind to PFCAs. By using PFCA-specific ELISA tests, researchers can accurately determine the precise concentration of PFCAs present in 3T3-L1 cells.

While this study helped answer many questions regarding information about the effects of shorter-chained PFCAs on humans, further studies are needed to verify the impacts of these PFCAs. Using 3T3-L1 preadipocytes is an effective initial step for evaluating the adipogenic potential of these PFCAS, however the cell model cannot accurately replicate the response that occurs within the human body.

Using human primary preadipocytes, we can more accurately represent the human physiology in an *in vitro* model. Their ability to differentiate in adipocytes is influenced by their location within the body (intra-abdominal/visceral or subcutaneous) and the characteristics of the donor (Lessard *et al.*, 2014). This can be valuable for studying obesity in individuals with varying ages, sex and other biological factors. The primary limitation concerning human primary preadipocytes is the restricted availability of donor tissue and the sparse cell yields obtained from biopsy material (Skurk *et al.*, 2007).

6.0 CONCLUSION

In conclusion, our study confirmed that PFOA, PFHpA, and PFHxA promote adipogenesis at high concentrations. This was evidenced by the upregulation of adipogenic markers *FABP4*, *LPL*, and *perilipin* in qPCR analysis and the accumulation of lipids within 3T3-L1 adipocytes. Specifically, PFHpA and PFHxA were postulated to induce adipogenesis primarily through the activation of PPARα, as these chemicals significantly activated PPARα but did not significantly activate PPARγ, however further confirmation is required. In contrast, PFOA significantly activated both PPARα and PPARγ, suggesting that adipogenesis may occur through both PPARα- and PPARγ-mediated pathways. Overall, this study contributes to a deeper

understanding of the biological effects of shorter-chained PFCAs, highlights the complexity of adipogenic regulation, emphasizes the need for comprehensive strategies to address the health and environmental challenges posed by these persistent chemicals.

APPENDICES

Table 1. Primers used for real time qPCR reactions

Primer	Forward Primer Sequence (Top) Reverse Primer Sequence (Bottom)	Tm(°C) Forward (Top) Reverse (Bottom)
m*ACOX1*	5'- CGC CGT CGA GAA ATC GAG AA -3' 5'- GTG CAC AGA GTT TTT AAA CCA CA -3'	57.3 54.2
mβ-Actin	5'- GAC TTC GAG CAA GAG ATG GC -3' 5'- CCA GAC AGC ACT GTG TTG GC -3'	55.8 59
m*CPT1b*	5'- AGG CAC TTC TCA GCA TGG TC -3' 5'- ACG GAC ACA GAT AGC CCA GA -3'	57.4 57.8
m*FABP4*	5'- GGA AGC TTG TCT CCA GTG AA -3' 5'- GCG GTG ATT TCA TCG AAT TC -3'	54.7 52.1
m*LPL*	5'- GAT CCG AGT GAA AGC CGG AG -3' 5'- TTG TTT GTC CAG TGT CAG CCA -3'	57.8 57.1
m*Perilipin*	5'- TTG GGG ATG GCC AAA GAG AC-3' 5'- CTC ACA AGG CTT GGT TTG GC -3'	57.5 57.1
m*UCP3*	5'- GGA CTT GGC CCA ACA TCA CA -3' 5'- TGA CAG GGG AAG TTG TCA GTA -3'	57.9 55.4

(A) **(B)**

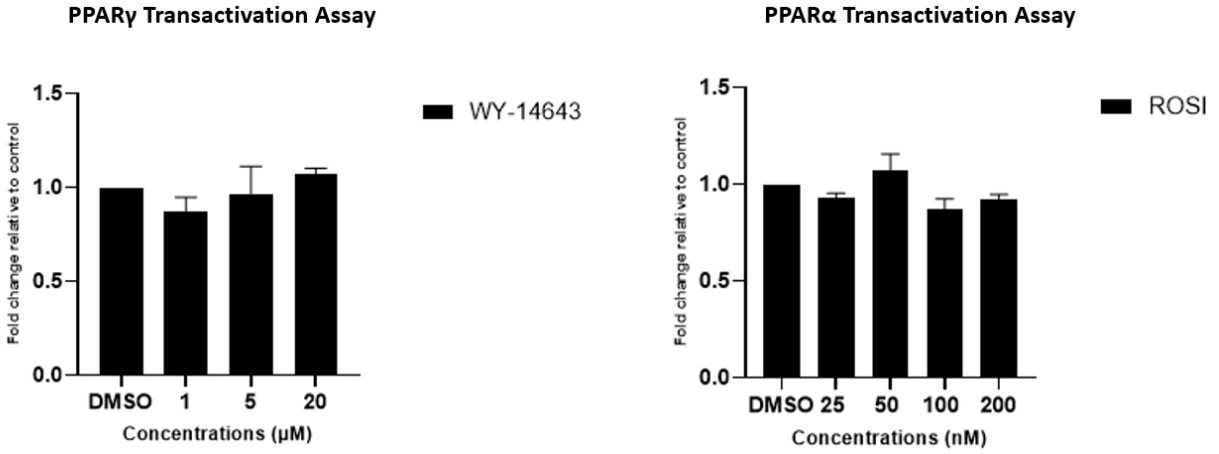

Supplemental Figure 1. PPARγ and PPAR-alpha transactivation assay data in the presence of increasing concentrations of WY-14643 and ROSI, respectfully. (A) WY-14643 treatments in PPARγ transactivation assay. (B) ROSI treatments in PPARα transactivation assay.

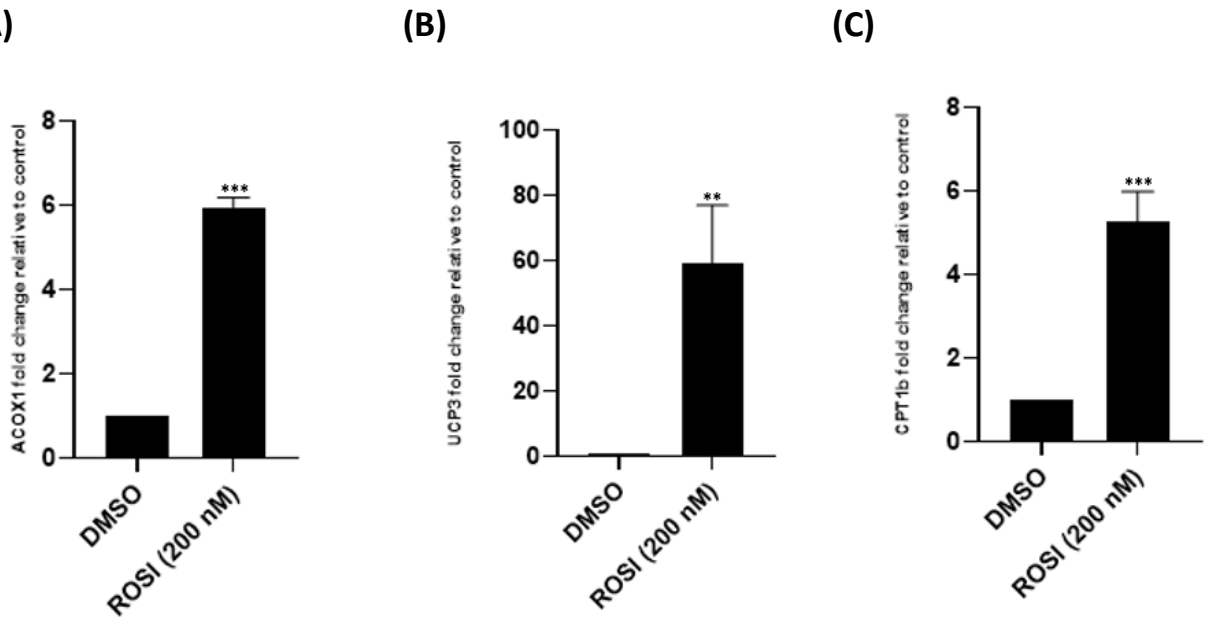

Supplemental Figure 2. Transcriptional expression analysis of genes involved in fatty acid oxidation of 3T3-L1 preadipocytes treated with ROSI at 200 nM. (A) ACOX1 expression, (B) UCP3 expression, and (C) CPT1b expression was looked at.

Table 2. Fold regulation of multiple genes involved in adipocyte differentiation and the maintenance of the mature adipocyte of 3T3-L1 preadipocytes treated with PFOA, PFHpA and PFHxA from concentrations ranging between 0-100 µM.

	Treatments							
Genes	ROSI (200 nM)	WY-14643 (20 µM)	PFOA (10 µM)	PFOA (100 µM)	PFHpA (25 µM)	PFHpA (100 µM)	PFHxA (25 µM)	PFHxA (100 µM)
Acacb	3.02	1.98	1.07	1.29	-1.13	1.18	-1.07	1.2
Adig	24.55	14.91	1.29	4.92	1.3	4.09	1.04	3.33
Adipoq	26.71	11.16	1.61	4.71	1.02	4.02	-1.03	2.48
Agt	4.91	2.05	-1.09	1.65	-1.3	1.54	-1.08	1.21
Ccnd1	-1.84	-1.24	1.01	-1.32	-1.09	-1.21	-1.2	1
Cdkn1a	2.07	1.07	-1.02	1.14	-1.25	1.03	-1.15	-1.08
Cebpa	5.61	3.62	-1.11	2.33	-1.23	2.07	-1.19	1.39
Cebpb	1.5	1.05	-1.26	-1	-1.69	-1.02	-1.24	-1.54
Cebpd	-1.67	-1.79	-1.06	-1.43	-1.6	-1.29	-1.2	-1.26
Cfd (adipsin)	37.36	9.57	1.29	2.78	1.09	2.88	-1.08	2.44
Dlk1	-2.79	-1.46	-1.32	-1.36	-1.54	-1.34	-1.73	-1.8
E2f1	-1.4	1.06	1.26	-1.26	1.17	-1.07	-1.04	1.26

Egr2	-1.55	-1.85	-1.31	-1.57	-1.61	-1.22	-1.59	-1.34
FABP4	30.44	22.53	1.33	6.66	1.32	5.47	1.04	3.47
Fasn	5.15	3.19	1.07	1.83	-1.11	1.73	-1.05	1.4
Fgf2	1.22	1.23	1.24	1.29	1.22	1.34	1.14	1.49
Foxc2	-1.4	-1.35	-1.22	1.04	-1.32	-1.04	-1.4	-1.31
Foxo1	1.87	1.59	1.31	1.27	1.22	1.35	1.11	1.47
Gata2	-2.91	-2.03	-1.02	-1.32	-1.2	-1.33	-1.16	-1.24
Gata3	1.25	-1.11	1.15	-1.04	-1.05	-1.09	-1.28	-1.08
Insr	2.37	1.37	-1.01	1.22	-1.24	1.14	-1.16	1.15
Irs2	2.65	1.81	-1.05	1.42	-1.26	1.38	-1.14	1.14
Klf15	17.52	5.08	-1.17	3.21	-1.14	2.49	1.02	2.35
Klf2	-1.98	-1.91	-1.61	-2.11	-2.22	-1.65	-1.74	-1.97
Lep	16.98	4.52	1.01	2.11	-1.14	1.34	-1.33	1.17
Lipe	17.05	6.48	-1.09	3.04	-1.27	2.49	-1.02	1.73
LPL	7.13	4.2	1.12	1.98	1.02	2.04	-1.02	1.74
Ncor2	1.08	-1.68	-1.04	-1.33	-1.52	-1.22	-1.41	-1.23
Nr0b2	-1.11	1.11	-1.3	-1.54	-1.8	-1.07	-3.19	-1.31
Nr1h3 (LXR-alpha)	11.61	6.24	1.09	2.77	1.01	2.56	1.01	2.07
Ppara	6.74	2.9	1.31	1.3	1.02	1.43	-1.08	1.41
Ppard	2.48	1.6	-1.06	1.33	-1.17	1.18	-1.18	-1.09
Pparg	7.53	3.81	-1.02	2.12	-1.02	2	-1.16	1.58
Ppargc1a	3.24	2.76	1.18	1.64	-1.14	1.6	-1.21	1.26
Ppargc1b	10.02	4.84	1.02	2.47	-1.14	2.25	-1.11	1.54
Prdm16	-1.05	1.45	1.03	-1.09	-1.44	-1.14	-2.27	1.03
Rb1	5.51	2.53	1.17	1.88	1.06	1.81	-1.04	1.51
Runx1t1	2.1	1.65	1.22	-1.26	-1.08	-1.32	-1.11	1.11
Sirt3	30.19	10.86	1.06	1.08	-1.05	1.1	-1.02	1.21
Slc2a4 (GLUT4)	-1.5	-1.55	1.04	4	-1.24	3.64	-1.11	2.07
Src	2.32	1.81	1.03	-1.18	-1.32	-1.19	-1.06	-1.04
Srebf1	1.4	1.39	1.11	1.33	-1	1.25	1	1.25
Taz	-1.54	-1.49	1.22	1.19	1.15	1.24	1.22	1.41
Twist1	-1.86	-1.39	1.04	-1.27	-1.14	-1.39	-1.14	-1.02
Vdr	-1.8	-1.57	1.01	-1.53	-1.16	-1.39	1.1	-1.11
Wnt10b	-1.80	-1.57	1.06	-1.06	-1.4	1.08	1.07	-1.02

Table 3. p-Values of multiple genes involved in adipocyte differentiation and the maintenance of the mature adipocyte of 3T3-L1 preadipocytes treated with PFOA, PFHpA and PFHxA from concentrations ranging between 0-100 µM. p-Values below 0.05 are highlighted in red font.

	Treatments							
Genes	ROSI (200 nM)	WY-14643 (20 µM)	PFOA (10 µM)	PFOA (100 µM)	PFHpA (25 µM)	PFHpA (100 µM)	PFHxA (25 µM)	PFHxA (100 µM)
Acacb	0.002103	0.031454	0.677095	0.293807	0.477628	0.380402	0.861755	0.04294
Adig	0.000153	0.001458	0.691566	0.06571	0.551504	0.095821	0.935391	0.076425
Adipoq	0.001469	0.015406	0.330933	0.075451	0.752542	0.118801	0.953465	0.183071
Agt	0.001715	0.068771	0.706399	0.181902	0.28977	0.262582	0.822945	0.700155
Ccnd1	0.017532	0.26352	0.922072	0.133643	0.88876	0.405313	0.459294	0.756778
Cdkn1a	0.085085	0.746259	0.908128	0.570565	0.276832	0.851781	0.51854	0.888756
Cebpa	0.006358	0.027938	0.658012	0.081151	0.627192	0.094296	0.490286	0.014474
Cebpb	0.068217	0.708776	0.146373	0.841313	0.027851	0.958836	0.39369	0.019715
Cebpd	0.012948	0.014455	0.77523	0.033557	0.000548	0.037633	0.186519	0.056706
Cfd (adipsin)	0.005866	0.043782	0.609542	0.16007	0.83715	0.112947	0.857018	0.820981
Dlk1	0.021301	0.016265	0.694327	0.186134	0.383741	0.317232	0.03034	0.384649
E2f1	0.159124	0.760171	0.410813	0.279622	0.477277	0.80165	0.987604	0.30375
Egr2	0.108294	0.190852	0.515145	0.074183	0.103678	0.335428	0.038446	0.033656
FABP4	0.000213	0.00676	0.61847	0.036492	0.541	0.068213	0.990634	0.188503
Fasn	0.008623	0.011376	0.776514	0.121935	0.670193	0.104364	0.822394	0.183071
Fgf2	0.306317	0.241234	0.412752	0.186026	0.286098	0.066947	0.340455	0.221154
Foxc2	0.065141	0.122954	0.149534	0.802027	0.135892	0.670205	0.043464	0.120581
Foxo1	0.023863	0.025738	0.123839	0.18634	0.327193	0.099672	0.55842	0.277715
Gata2	0.009714	0.035647	0.84905	0.161738	0.179307	0.17026	0.351771	0.820401
Gata3	0.456609	0.749319	0.647624	0.700199	0.703149	0.573893	0.35408	0.447066
Insr	0.006773	0.130137	0.960714	0.18456	0.235342	0.383757	0.285665	0.860007
Irs2	0.058693	0.081793	0.745466	0.233561	0.374422	0.289289	0.670624	0.785533
Klf15	0.000018	0.008719	0.565164	0.098795	0.66983	0.056894	0.806035	0.07658
Klf2	0.03327	0.025175	0.048209	0.032551	0.016226	0.051608	0.05869	0.825518
Lep	0.00005	0.048137	0.748067	0.192824	0.943595	0.460472	0.247264	0.054998
Lipe	0.000027	0.037173	0.657633	0.076225	0.625879	0.152419	0.970142	0.858324
LPL	0.005204	0.018794	0.801254	0.15078	0.893636	0.141416	0.93725	0.985894
Ncor2	0.599538	0.03101	0.891458	0.070681	0.022435	0.271723	0.073579	0.687551
Nr0b2	0.913308	0.757458	0.591885	0.553671	0.887981	0.741476	0.109187	0.089438
Nr1h3 (LXR-alpha)	0.000128	0.009677	0.829775	0.096442	0.892923	0.097188	0.944266	0.60566
Ppara	0.055938	0.049599	0.504878	0.443707	0.817716	0.26738	0.694352	0.43337
Ppard	0.006892	0.009099	0.735982	0.150128	0.256476	0.289447	0.549517	0.115565
Pparg	0.004317	0.032236	0.8138	0.124184	0.964969	0.089023	0.521494	0.482209

Ppargc1a	0.002386	0.029964	0.600891	0.175296	0.874648	0.187223	0.567698	0.190024
Ppargc1b	0.001805	0.013658	0.832647	0.063123	0.789195	0.116271	0.717303	0.826169
Prdm16	0.892241	0.352734	0.513054	0.850775	0.93511	0.926013	0.08437	0.057661
Rb1	0.026382	0.0048	0.368983	0.045894	0.7277	0.025648	0.685717	0.276606
Runx1t1	0.019981	0.049972	0.417969	0.256339	0.545077	0.234905	0.446119	0.333146
Sirt3	0.040882	0.098704	0.721619	0.614616	0.77129	0.592801	0.921505	0.053798
Slc2a4 (GLUT4)	0.003253	0.041182	0.967787	0.09565	0.673184	0.109031	0.844805	0.737886
Src	0.06581	0.002667	0.787323	0.266589	0.016439	0.070387	0.714327	0.254496
Srebf1	0.001686	0.020848	0.451845	0.14751	0.922029	0.244624	0.9981	0.238273
Taz	0.087514	0.066332	0.201378	0.383685	0.416051	0.268151	0.20641	0.186778
Twist1	0.006277	0.028588	0.736635	0.053452	0.18665	0.051798	0.474991	0.183071
Vdr	0.254628	0.469444	0.882518	0.26474	0.624251	0.40126	0.800698	0.036922
Wnt10b	0.074575	0.114033	0.897564	0.669009	0.682182	0.780426	0.846586	0.183071

REFERENCES

Agard-Jones, V. (2014, May 27). *Spray*. Somatosphere. https://somatosphere.com/2014/spray.html/

Alabdulkarim, B., Bakeet, Z. A. N., & Arzoo, S. (2012). Role of some functional lipids in preventing diseases and promoting health. *Journal of King Saud University. Science*, *24*(4), 319–329. https://doi.org/10.1016/j.jksus.2012.03.001

Ali, A. T., Hochfeld, W. E., Myburgh, R., & Pepper, M. S. (2013). Adipocyte and adipogenesis. *European Journal of Cell Biology*, *92*(6–7), 229–236. https://doi.org/10.1016/j.ejcb.2013.06.001

Almeida, N. M. S., Eken, Y., & Wilson, A. K. (2021). Binding of Per- and Polyfluoro-alkyl Substances to Peroxisome Proliferator-Activated Receptor Gamma. *ACS Omega*, *6*(23), 15103–15114. https://doi.org/10.1021/acsomega.1c01304

Al-Nasiry, S., Geusens, N., Hanssens, M., Luyten, C., & Pijnenborg, R. (2007). The use of Alamar Blue assay for quantitative analysis of viability, migration and invasion of choriocarcinoma cells. *Human Reproduction (Oxford)*, *22*(5), 1304–1309. https://doi.org/10.1093/humrep/dem011

Azizi, L., Turkki, P., Huynh, N., Massera, J. M., & Hytönen, V. P. (2021). Surface Modification of Bioactive Glass Promotes Cell Attachment and Spreading. *ACS Omega*, *6*(35), 22635–22642. https://doi.org/10.1021/acsomega.1c02669

Beggs, K. M., McGreal, S. R., McCarthy, A., Gunewardena, S., Lampe, J. N., Lau, C., & Apte, U. (2016). The role of hepatocyte nuclear factor 4-alpha in perfluorooctanoic acid- and perfluorooctanesulfonic acid-induced hepatocellular dysfunction. *Toxicology and Applied Pharmacology*, *304*, 18–29. https://doi.org/10.1016/j.taap.2016.05.001

Behr, A.-C., Plinsch, C., Braeuning, A., & Buhrke, T. (2020). Activation of human nuclear receptors by perfluoroalkylated substances (PFAS). *Toxicology in Vitro*, *62*, 104700-. https://doi.org/10.1016/j.tiv.2019.104700

Björklund, J. A., Thuresson, K., & de Wit, C. A. (2009). Perfluoroalkyl Compounds (PFCs) in Indoor Dust: Concentrations, Human Exposure Estimates, and Sources. *Environmental Science & Technology*, *43*(7), 2276–2281. https://doi.org/10.1021/es803201a

Bogdanov, M., Mileykovskaya, E., & Dowhan, W. (2008). Lipids in the Assembly of Membrane Proteins and Organization of Protein Supercomplexes: Implications for Lipid-linked Disorders. *Lipids in Health and Disease*, 197–239. https://doi.org/10.1007/978-1-4020-8831-5_8

Brocker, C. N., Yue, J., Kim, D., Qu, A., Bonzo, J. A., & Gonzalez, F. J. (2017). Hepatocyte-specific PPARA expression exclusively promotes agonist-induced cell proliferation

without influence from nonparenchymal cells. *American Journal of Physiology: Gastrointestinal and Liver Physiology*, *312*(3), G283–G299. https://doi.org/10.1152/ajpgi.00205.2016

Brun, R. P., Tontonoz, P., Forman, B. M., Ellis, R., Chen, J., Evans, R. M., & Spiegelman, B. M. (1996). Differential activation of adipogenesis by multiple PPAR isoforms. *Genes & Development*, *10*(8), 974–984. https://doi.org/10.1101/gad.10.8.974

BSI, C. (2009). Water quality− Determination of perfluorooctanesulfonate (PFOS) and perfluorooctanoate (PFOA)− Method for unfiltered samples using solid-phase extraction and liquid chromatography/mass spectrometry. *BS ISO 25101*

Buck, R. C., Franklin, J., Berger, U., Conder, J. M., Cousins, I. T., de Voogt, P., Jensen, A. A., Kannan, K., Mabury, S. A., & van Leeuwen, S. P. (2011). Perfluoroalkyl and polyfluoroalkyl substances in the environment: Terminology, classification, and origins. *Integrated Environmental Assessment and Management*, *7*(4), 513–541. https://doi.org/10.1002/ieam.258

Campo, J., Masiá, A., Picó, Y., Farré, M., & Barceló, D. (2014). Distribution and fate of perfluoroalkyl substances in Mediterranean Spanish sewage treatment plants. *The Science of the Total Environment*, *472*, 912–922. https://doi.org/10.1016/j.scitotenv.2013.11.056

Campo, J., Masiá, A., Picó, Y., Farré, M., & Barceló, D. (2014). Distribution and fate of perfluoroalkyl substances in Mediterranean Spanish sewage treatment plants. *The Science of the Total Environment*, *472*, 912–922. https://doi.org/10.1016/j.scitotenv.2013.11.056

Carpentier, A. C., Blondin, D. P., Haman, F., & Richard, D. (2023). Brown Adipose Tissue—A Translational Perspective. *Endocrine Reviews*, *44*(2), 143–192. https://doi.org/10.1210/endrev/bnac015

Castro, R. (2022, December 7). *Hyperinsulinemia: Is it diabetes?* Mayo Clinic. https://www.mayoclinic.org/diseases-conditions/type-2-diabetes/expert-answers/hyperinsulinemia/faq-20058488#:~:text=Hyperinsulinemia%20(hi%2Dpur%2Din

CDC. (2024, May 13). *About Insulin Resistance and Type 2 Diabetes*. Diabetes. https://www.cdc.gov/diabetes/about/insulin-resistance-type-2-diabetes.html

Cedikova, M., Kripnerová, M., Dvorakova, J., Pitule, P., Grundmanova, M., Babuska, V., Mullerova, D., & Kuncova, J. (2016). Mitochondria in White, Brown, and Beige Adipocytes. *Stem Cells International*, *2016*, 6067349–11. https://doi.org/10.1155/2016/6067349

CHANDRA, V., PENGXIANG HUANG, HAMURO, Y., RAGHURAM, S., YONGJUN WANG, BURRIS, T. P., & RASTINEJAD, F. (2008). Structure of the intact PPAR-γ-RXR-α nuclear receptor complex on DNA. *Nature (London)*, *456*(7220), 350–356. https://doi.org/10.1038/nature07413

Chang, C.-S., Tsai, P.-J., Sung, J.-M., Chen, J.-Y., Ho, L.-C., Pandya, K., Maeda, N., & Tsai, Y.-S. (2014). Diuretics Prevent Thiazolidinedione-Induced Cardiac Hypertrophy without Compromising Insulin-Sensitizing Effects in Mice. *The American Journal of Pathology*, *184*(2), 442–453. https://doi.org/10.1016/j.ajpath.2013.10.020

ChemSec identifies the top 12 PFAS producers in the world and reveals shocking societal costs. (2023, May 23). Https://Chemsec.org/Chemsec-Identifies-The-Top-12-Pfas-Producers-In-The-World-And-Reveals-Shocking-Societal-Costs/#_ftnref1. https://chemsec.org/chemsec-identifies-the-top-12-pfas-producers-in-the-world-and-reveals-shocking-societal-costs/#_ftnref1

Chen, T., Ma, F., Peng, Y., Sun, R., Xi, Q., Sun, J., Zhang, J., Zhang, Y., & Li, M. (2022). Plant miR167e-5p promotes 3T3-L1 adipocyte adipogenesis by targeting β-catenin. *In Vitro Cellular & Developmental Biology. Animal*, *58*(6), 471–479. https://doi.org/10.1007/s11626-022-00702-w

Chen, Y., Wu, Y., Lv, J., Zhou, S., Lin, S., Huang, S., Zheng, L., Deng, G., Feng, Y., Zhang, G., & Feng, W. (2024). Overall and individual associations between per- and polyfluoroalkyl substances and liver function indices and the metabolic mechanism. *Environment International*, *183*, 108405–108405. https://doi.org/10.1016/j.envint.2023.108405

Christofides, A., Konstantinidou, E., Jani, C., & Boussiotis, V. A. (2021). The role of peroxisome proliferator-activated receptors (PPAR) in immune responses. *Metabolism, Clinical and Experimental*, *114*, 154338–154338. https://doi.org/10.1016/j.metabol.2020.154338

Church, C., Horowitz, M., & Rodeheffer, M. (2012). WAT is a functional adipocyte? *Adipocyte*, *1*(1), 38–45. https://doi.org/10.4161/adip.19132

Cinti, S. (2012). The adipose organ at a glance. *Disease Models & Mechanisms*, *5*(5), 588–594. https://doi.org/10.1242/dmm.009662

Coelho, M., Oliveira, T., & Fernandes, R. (2013). Biochemistry of adipose tissue: an endocrine organ. *Archives of Medical Science*, *9*(2), 191–200. https://doi.org/10.5114/aoms.2013.33181

Combarnous, Y., & Nguyen, T. M. D. (2019). Comparative Overview of the Mechanisms of Action of Hormones and Endocrine Disruptor Compounds. *Toxics (Basel)*, *7*(1), 5-. https://doi.org/10.3390/toxics7010005

D'Aiuto, F., & Suvan, J. (2012). Obesity, Inflammation, and Oral Infections: Are microRNAs the Missing Link? *Journal of Dental Research*, *91*(1), 5–7. https://doi.org/10.1177/0022034511427164

Dabelea, D., Mayer-Davis, E. J., Lamichhane, A. P., D'Agostino, R. B. J., Liese, A. D., Vehik, K. S., Narayan, K. M. V., Zeitler, P., & Hamman, R. F. (2008). Association of Intrauterine Exposure to Maternal Diabetes and Obesity With Type 2 Diabetes in Youth:

The SEARCH Case-Control Study. *Diabetes Care*, *31*(7), 1422–1426. https://doi.org/10.2337/dc07-2417

David, N., Antignac, J.-P., Roux, M., Marchand, P., Michalak, S., Oberti, F., Fouchard, I., Lannes, A., Blanchet, O., Cales, P., Blanc, E. B., Boursier, J., & Canivet, C. M. (2023). Associations between perfluoroalkyl substances and the severity of non-alcoholic fatty liver disease. *Environment International*, *180*, 108235–108235. https://doi.org/10.1016/j.envint.2023.108235

de Sá, P. M., Richard, A. J., Hang, H., & Stephens, J. M. (2017). Transcriptional Regulation of Adipogenesis. *Comprehensive Physiology*, *7*(2), 635–674. https://doi.org/10.1002/cphy.c160022

Degerman, E., Landström, T. R., Wijkander, J., Holst, L. S., Ahmad, F., Belfrage, P., & Manganiello, V. (1998). Phosphorylation and Activation of Hormone-Sensitive Adipocyte Phosphodiesterase Type 3B. *Methods (San Diego, Calif.)*, *14*(1), 43–53. https://doi.org/10.1006/meth.1997.0564

Domingo J. L. (2012). Health risks of dietary exposure to perfluorinated compounds. *Environment international*, *40*, 187–195. https://doi.org/10.1016/j.envint.2011.08.001

Edwards, M., & Mohiuddin, S. S. (2023). *Biochemistry, Lipolysis*. PubMed; StatPearls Publishing. https://www.ncbi.nlm.nih.gov/books/NBK560564/#:~:text=Introduction

Egeghy, P. P., & Lorber, M. (2011). An assessment of the exposure of Americans to perfluorooctane sulfonate: A comparison of estimated intake with values inferred from NHANES data. *Journal of Exposure Science & Environmental Epidemiology*, *21*(2), 150–168. https://doi.org/10.1038/jes.2009.73

El-Jack, A. K., Hamm, J. K., Pilch, P. F., & Farmer, S. R. (1999). Reconstitution of Insulin-sensitive Glucose Transport in Fibroblasts Requires Expression of Both PPARγ and C/EBPα. *The Journal of Biological Chemistry*, *274*(12), 7946–7951. https://doi.org/10.1074/jbc.274.12.7946

Evans, N., Conley, J. M., Cardon, M., Hartig, P., Medlock-Kakaley, E., & Gray, L. E. (2022). In vitro activity of a panel of per- and polyfluoroalkyl substances (PFAS), fatty acids, and pharmaceuticals in peroxisome proliferator-activated receptor (PPAR) alpha, PPAR gamma, and estrogen receptor assays. *Toxicology and Applied Pharmacology*, *449*, 116136–116136. https://doi.org/10.1016/j.taap.2022.116136

Evans, N., Conley, J. M., Cardon, M., Hartig, P., Medlock-Kakaley, E., & Gray, L. E. (2022). In vitro activity of a panel of per- and polyfluoroalkyl substances (PFAS), fatty acids, and pharmaceuticals in peroxisome proliferator-activated receptor (PPAR) alpha, PPAR gamma, and estrogen receptor assays. *Toxicology and Applied Pharmacology*, *449*, 116136–116136. https://doi.org/10.1016/j.taap.2022.116136

Fei, C., McLaughlin, J. K., Lipworth, L., & Olsen, J. (2009). Maternal levels of perfluorinated chemicals and subfecundity. *Human Reproduction (Oxford), 24*(5), 1200–1205. https://doi.org/10.1093/humrep/den490

Filipovic, M., Woldegiorgis, A., Norström, K., Bibi, M., Lindberg, M., & Österås, A.-H. (2015). Historical usage of aqueous film forming foam: A case study of the widespread distribution of perfluoroalkyl acids from a military airport to groundwater, lakes, soils and fish. *Chemosphere (Oxford), 129*, 39–45. https://doi.org/10.1016/j.chemosphere.2014.09.005

Freeman, A. M., Acevedo, L. A., & Pennings, N. (2023). *Insulin Resistance*. PubMed; StatPearls Publishing. https://www.ncbi.nlm.nih.gov/books/NBK507839/#:~:text=Insulin%20resistance%2C%20identified%20as%20an

Fruh, S. M. (2017). Obesity: Risk factors, complications, and strategies for sustainable long-term weight management. *J. Am. Assoc. Nurse Pract.* doi:10.1002/2327-6924.12510.

Furuhashi, M., Saitoh, S., Shimamoto, K., & Miura, T. (2014). Fatty Acid-Binding Protein 4 (*FABP4*): Pathophysiological Insights and Potent Clinical Biomarker of Metabolic and Cardiovascular Diseases. *Clinical Medicine Insights. Cardiology*, *2014*(S3), 23–33. https://doi.org/10.4137/CMC.S17067

Galic, S., Oakhill, J. S., & Steinberg, G. R. (2010). Adipose tissue as an endocrine organ. *Molecular and Cellular Endocrinology, 316*(2), 129–139. https://doi.org/10.1016/j.mce.2009.08.018

GARIN-SHKOLNIK, T., RUDICH, A., HOTAMISLIGIL, G. S., & RUBINSTEIN, M. (2014). *FABP4* Attenuates PPARγ and Adipogenesis and Is Inversely Correlated With PPARγ in Adipose Tissues. *Diabetes (New York, N.Y.)*, *63*(3), 900–911. https://doi.org/10.2337/db13-0436

Goodrow, S. M., Ruppel, B., Lippincott, R. L., Post, G. B., & Procopio, N. A. (2020). Investigation of levels of perfluoroalkyl substances in surface water, sediment and fish tissue in New Jersey, USA. *The Science of the Total Environment*, *729*, 138839–138839. https://doi.org/10.1016/j.scitotenv.2020.138839

Gore, A. C., Chappell, V. A., Fenton, S. E., Flaws, J. A., Nadal, A., Prins, G. S., Toppari, J., & Zoeller, R. T. (2015). EDC-2: The Endocrine Society's Second Scientific Statement on Endocrine-Disrupting Chemicals. *Endocrine Reviews*, *36*(6), E1–E150. https://doi.org/10.1210/er.2015-1010

Government of Canada, S. C. (2024, March 4). *An overview of weight and height measurements on World Obesity Day*. Www.statcan.gc.ca. https://www.statcan.gc.ca/o1/en/plus/5742-overview-weight-and-height-measurements-world-obesity-day

Grün, F. (2010). Obesogens. *Current Opinion in Endocrinology, Diabetes and Obesity, 17* (5), 453-459. doi: 10.1097/MED.0b013e32833ddea0.

Grün, F., & Blumberg, B. (2006). Environmental Obesogens: Organotins and Endocrine Disruption via Nuclear Receptor Signaling. *Endocrinology (Philadelphia)*, *147*(6), s50–s55. https://doi.org/10.1210/en.2005-1129

Gyamfi, D., Ofori Awuah, E., & Owusu, S. (2019). *Chapter 2 - Lipid Metabolism: An Overview* (V. B. Patel, Ed.). ScienceDirect; Academic Press. https://www.sciencedirect.com/science/article/abs/pii/B9780128112977000020?via%3Dihub

Hall, S. M., Patton, S., Petreas, M., Zhang, S., Phillips, A. L., Hoffman, K., & Stapleton, H. M. (2020). Per- and Polyfluoroalkyl Substances in Dust Collected from Residential Homes and Fire Stations in North America. *Environmental Science & Technology*, *54*(22), 14558–14567. https://doi.org/10.1021/acs.est.0c04869

Hansen, K. J., Johnson, H. O., Eldridge, J. S., Butenhoff, J. L., & Dick, L. A. (2002). Quantitative Characterization of Trace Levels of PFOS and PFOA in the Tennessee River. *Environmental Science & Technology*, *36*(8), 1681–1685. https://doi.org/10.1021/es010780r

Hellsing, M. S., Josefsson, S., Hughes, A. V., & Ahrens, L. (2016). Sorption of perfluoroalkyl substances to two types of minerals. *Chemosphere (Oxford)*, *159*, 385–391. https://doi.org/10.1016/j.chemosphere.2016.06.016

Henderson, G. C. (2021). Plasma Free Fatty Acid Concentration as a Modifiable Risk Factor for Metabolic Disease. *Nutrients*, *13*(8), 2590-. https://doi.org/10.3390/nu13082590

Hiller-Sturmhöfel, S., & Bartke, A. (1998). The endocrine system: an overview. *Alcohol health and research world*, *22*(3), 153–164.

Hishida, T., Nishizuka, M., Osada, S., & Imagawa, M. (2009). The role of C/EBPδ in the early stages of adipogenesis. *Biochimie*, *91*(5), 654–657. https://doi.org/10.1016/j.biochi.2009.02.002

Horwitz, A., & Birk, R. (2023). Adipose Tissue Hyperplasia and Hypertrophy in Common and Syndromic Obesity-The Case of BBS Obesity. *Nutrients*, *15*(15), 3445-. https://doi.org/10.3390/nu15153445

Huang, W., Ai, W., Lin, W., Fang, F., Wang, X., Huang, H., Dahlgren, R. A., & Wang, H. (2020). Identification of receptors for eight endocrine disrupting chemicals and their underlying mechanisms using zebrafish as a model organism. *Ecotoxicology and Environmental Safety*, *204*, 111068–111068. https://doi.org/10.1016/j.ecoenv.2020.111068

Hughlett, M. & Johnson, C. (2022, December 21). *3M to end manufacture and use of harmful PFAS by 2025*. Wisconsin Watch. https://wisconsinwatch.org/2022/12/3m-to-end-manufacture-and-use-of-harmful-pfas-by 2025/#:~:text=3M%20will%20%E2%80%9Cwork%20to%20discontinue

IJpenberg, A., Jeannin, E., Wahli, W., & Desvergne, B. (1997). Polarity and specific sequence requirements of peroxisome proliferator-activated receptor (PPAR)/retinoid X receptor heterodimer binding to DNA. A functional analysis of the malic enzyme gene PPAR response element. *The Journal of Biological Chemistry*, *272*(32), 20108–20117. https://doi.org/10.1074/jbc.272.32.20108

Jakab, J., Miskic, B., Miksic, S., Juranic, B., Cosic, V., Schwarz, D., & Vcev, A. (2021). Adipogenesis as a Potential Anti-Obesity Target: A Review of Pharmacological Treatment and Natural Products. *Diabetes, Metabolic Syndrome and Obesity*, *13*, 67-. https://doi.org/10.2l47/DMSO.S281186

Jia, X., Li, X., Zhou, L., Hui, Y., Li, W., Cai, Y., & Shi, Y. (2023). Variations of the Level, Profile, and Distribution of PFAS around POSF Manufacturing Facilities in China: An Overlooked Source of PFCA. *Environmental Science & Technology*, *57*(13), 5264–5274. https://doi.org/10.1021/acs.est.2c08995

Kahn, C. R., Taniguchi, C. M., & Emanuelli, B. (2006). Critical nodes in signalling pathways: insights into insulin action. *Nature Reviews. Molecular Cell Biology*, *7*(2), 85–96. https://doi.org/10.1038/nrm1837

Kelesidis, T. (2010). Narrative Review: The Role of Leptin in Human Physiology: Emerging Clinical Applications. *Annals of Internal Medicine*, *152*(2), 93–100. https://doi.org/10.7326/0003-4819-152-2-201001190-00008

Khan, M., & Joseph, F. (2014). Adipose Tissue and Adipokines: The Association with and Application of Adipokines in Obesity. *Scientifica (Cairo)*, *2014*, 328592–328597. https://doi.org/10.1155/2014/328592

Kim, S., Ha, J. M., Yun, S. J., Kim, E. K., Chung, S. W., Hong, K. W., Kim, C. D., & Bae, S. S. (2010). Transcriptional activation of peroxisome proliferator-activated receptor-γ requires activation of both protein kinase A and Akt during adipocyte differentiation. *Biochemical and Biophysical Research Communications*, *399*(1), 55–59. https://doi.org/10.1016/j.bbrc.2010.07.038

Knutsen, H. K., Alexander, J., Barregård, L., Bignami, M., Brüschweiler, B., Ceccatelli, S., Cottrill, B., Dinovi, M., Edler, L., Grasl-Kraupp, B., Hogstrand, C., Hoogenboom, L. (Ron), Nebbia, C. S., Oswald, I. P., Petersen, A., Rose, M., Roudot, A., Vleminckx, C., Vollmer, G., … Schwerdtle, T. (2018). Risk to human health related to the presence of perfluorooctane sulfonic acid and perfluorooctanoic acid in food. *EFSA Journal*, *16*(12), e05194-n/a. https://doi.org/10.2903/j.efsa.2018.5194

Krey, G., Keller, H., Mahfoudi, A., Medin, J., Ozato, K., Dreyer, C., & Wahli, W. (1993). Xenopus peroxisome proliferator activated receptors: Genomic organization, response element recognition, heterodimer formation with retinoid X receptor and activation by fatty acids. *Journal of Steroid Biochemistry and Molecular Biology*, *47*(1), 65–73. https://doi.org/10.1016/0960-0760(93)90058-5

Kubota, N., Terauchi, Y., Miki, H., Tamemoto, H., Yamauchi, T., Komeda, K., Satoh, S., Nakano, R., Ishii, C., Sugiyama, T., Eto, K., Tsubamoto, Y., Okuno, A., Murakami, K., Sekihara, H., Hasegawa, G., Naito, M., Toyoshima, Y., Tanaka, S., … Kadowaki, T. (1999). PPARγ Mediates High-Fat Diet–Induced Adipocyte Hypertrophy and Insulin Resistance. *Molecular Cell*, *4*(4), 597–609. https://doi.org/10.1016/S1097-2765(00)80210-5

Langston, N. (2010). *Toxic bodies hormone disruptors and the legacy of DES* (1st ed.). Yale University Press. https://doi.org/10.12987/9780300162998
Langston, N. (2010). *Toxic bodies hormone disruptors and the legacy of DES* (1st ed.). Yale University Press. https://doi.org/10.12987/9780300162998
Lefebvre, P., Chinetti, G., Fruchart, J.-C., & Staels, B. (2006). Sorting out the roles of PPAR alpha in energy metabolism and vascular homeostasis. *The Journal of Clinical Investigation*, *116*(3), 571–580. https://doi.org/10.1172/JCI27989

Legislative Services Branch. (2024). *Prohibition of Certain Toxic Substances Regulations, 2012*. Justice.gc.ca. https://laws-lois.justice.gc.ca/eng/regulations/SOR-2012-285/page-1.html

Lessard, J. et al. (2014). Low abdominal subcutaneous preadipocyte adipogenesis is associated with visceral obesity, visceral adipocyte hypertrophy, and a dysmetabolic state. Adipocyte 3, 197–205.

Lidell, M. E., & Enerbäck, S. (2015). Brown adipose tissue and bone.(White, Beige, Brown: What Determines the Colour of Adipose Tissue). *International Journal of Obesity*, *5*(S1), S23-. https://doi.org/10.1038/ijosup.2015.7

Lin, X., & Li, H. (2021). Obesity: Epidemiology, Pathophysiology, and Therapeutics. *Frontiers in Endocrinology (Lausanne)*, *12*, 706978–706978. https://doi.org/10.3389/fendo.2021.706978

Liu, S., Anderson, P. J., Rajagopal, S., Lefkowitz, R. J., & Rockman, H. A. (2024). G Protein-Coupled Receptors: A Century of Research and Discovery. *Circulation Research*, *135*(1), 174-. https://doi.org/10.1161/CIRCRESAHA.124.323067

Liu, Y., Jiang, L., Wang, H., Wang, H., Jiao, W., Chen, G., Zhang, P., Hui, D., & Jian, X. (2019). A brief review for fluorinated carbon: synthesis, properties and applications. *Nanotechnology Reviews (Berlin)*, *8*(1), 573–586. https://doi.org/10.1515/ntrev-2019-0051

Llorca, M., Schirinzi, G., Martínez, M., Barceló, D., & Farré, M. (2018). Adsorption of perfluoroalkyl substances on microplastics under environmental conditions. *Environmental Pollution (1987)*, *235*, 680–691. https://doi.org/10.1016/j.envpol.2017.12.075

Louis, G. M. B., Chen, Z., Schisterman, E. F., Kim, S., Sweeney, A. M., Sundaram, R., Lynch, C. D., Gore-Langton, R. E., & Barr, D. B. (2015). Perfluorochemicals and human semen

quality: the LIFE study. *Environmental Health Perspectives*, *123*(1), 57–63. https://doi.org/10.1289/ehp.1307621

Luo, L., & Liu, M. (2016). Adipose tissue in control of metabolism. *The Journal of Endocrinology*, *231*(3), R77–R99. https://doi.org/10.1530/JOE-16-0211

Ma, Y., Yang, J., Wan, Y., Peng, Y., Ding, S., Li, Y., Xu, B., Chen, X., Xia, W., Ke, Y., & Xu, S. (2018). Low-level perfluorooctanoic acid enhances 3 T3-L1 preadipocyte differentiation via altering peroxisome proliferator activated receptor gamma expression and its promoter DNA methylation. *Journal of Applied Toxicology*, *38*(3), 398–407. https://doi.org/10.1002/jat.3549

Mangelsdorf, D. J., Thummel, C., Beato, M., Herrlich, P., Schütz, G., Umesono, K., Blumberg, B., Kastner, P., Mark, M., Chambon, P., & Evans, R. M. (1995). The nuclear receptor superfamily: The second decade. *Cell*, *83*(6), 835–839. https://doi.org/10.1016/0092-8674(95)90199-X

McGarry, J. D., & Brown, N. F. (1997). The Mitochondrial Carnitine Palmitoyltransferase System — From Concept to Molecular Analysis. *European Journal of Biochemistry*, *244*(1), 1–14. https://doi.org/10.1111/j.1432-1033.1997.00001.x

Melzer, D., Rice, N., Depledge, M. H., Henley, W. E., & Galloway, T. S. (2010). Association between Serum Perfluorooctanoic Acid (PFOA) and Thyroid Disease in the U.S. National Health and Nutrition Examination Survey. *Environmental Health Perspectives*, *118*(5), 686–692. https://doi.org/10.1289/ehp.0901584

Moseti, D., Regassa, A., & Kim, W.-K. (2016). Molecular Regulation of Adipogenesis and Potential Anti-Adipogenic Bioactive Molecules. *International Journal of Molecular Sciences*, *17*(1), 124–124. https://doi.org/10.3390/ijms17010124

Muir, L. A., Neeley, C. K., Meyer, K. A., Baker, N. A., Brosius, A. M., Washabaugh, A. R., Varban, O. A., Finks, J. F., Zamarron, B. F., Flesher, C. G., Chang, J. S., DelProposto, J. B., Geletka, L., Martinez-Santibanez, G., Kaciroti, N., Lumeng, C. N., & O'Rourke, R. W. (2016). Adipose tissue fibrosis, hypertrophy, and hyperplasia: Correlations with diabetes in human obesity. *Obesity (Silver Spring, Md.)*, *24*(3), 597–605. https://doi.org/10.1002/oby.21377

OECD. 2013. OECD/UNEP Global PFC Group, Synthesis paper on per- and polyfluorinated chemicals (PFCs). Paris: Health and Safety Environment, Environment Directorate, OECD. https://www.oecd.org/env/ehs/risk-management/PFC_FINAL-Web.pdf

Olsen, G. W., Hansen, K. J., Stevenson, L. A., Burris, J. M., & Mandel, J. H. (2003). Human Donor Liver and Serum Concentrations of Perfluorooctanesulfonate and Other Perfluorochemicals. *Environmental Science & Technology*, *37*(5), 888–891. https://doi.org/10.1021/es020955c

Panieri, E., Baralic, K., Djukic-Cosic, D., Buha Djordjevic, A., & Saso, L. (2022). PFAS Molecules: A Major Concern for the Human Health and the Environment. *Toxics (Basel), 10*(2), 44-. https://doi.org/10.3390/toxics10020044

Panuganti, K. K., Nguyen, M. & Kshirsagar, R. K. (2022). *Obesity*.

Payne, A. H., & Hales, D. B. (2004). Overview of Steroidogenic Enzymes in the Pathway from Cholesterol to Active Steroid Hormones. *Endocrine Reviews*, *25*(6), 947–970. https://doi.org/10.1210/er.2003-0030

Pegoraro, G., & Misteli, T. (2017). High-Throughput Imaging for the Discovery of Cellular Mechanisms of Disease. *Trends in Genetics*, *33*(9), 604–615. https://doi.org/10.1016/j.tig.2017.06.005

Peshdary, V., Calzadilla, G., Landry, A., Sorisky, A., & Atlas, E. (2019). Dechlorane Plus increases adipogenesis in 3T3-L1 and human primary preadipocytes independent of peroxisome proliferator-activated receptor [gamma] transcriptional activity. *International Journal of Obesity*, *43*(3), 545-. https://doi.org/10.1038/s41366-018-0072-7

Poothong, S., Padilla-Sánchez, J. A., Papadopoulou, E., Giovanoulis, G., Thomsen, C., & Haug, L. S. (2019). Hand Wipes: A Useful Tool for Assessing Human Exposure to Poly- and Perfluoroalkyl Substances (PFASs) through Hand-to-Mouth and Dermal Contacts. *Environmental Science & Technology*, *53*(4), 1985–1993. https://doi.org/10.1021/acs.est.8b05303

Poothong, S., Papadopoulou, E., Padilla-Sánchez, J. A., Thomsen, C., & Haug, L. S. (2020). Multiple pathways of human exposure to poly- and perfluoroalkyl substances (PFASs): From external exposure to human blood. *Environment International*, *134*, 105244-. https://doi.org/10.1016/j.envint.2019.105244

Poulos, S. P., Dodson, M. V., & Hausman, G. J. (2010). Cell line models for differentiation: preadipocytes and adipocytes. *Experimental Biology and Medicine*, *235*(10), 1185–1193. https://doi.org/10.1258/ebm.2010.010063

Qiu, Z., Wei, Y., Chen, N., Jiang, M., Wu, J., & Liao, K. (2001). DNA Synthesis and Mitotic Clonal Expansion Is Not a Required Step for 3T3-L1 Preadipocyte Differentiation into Adipocytes. *The Journal of Biological Chemistry*, *276*(15), 11988–11995. https://doi.org/10.1074/jbc.M011729200

Quintanilla Rodriguez, B. S., & Correa, R. (2022). *ROSI*. PubMed; StatPearls https://www.ncbi.nlm.nih.gov/books/NBK544230/#:~:text=ROSI%20is%20a%20medication%20used

Ramírez Carnero, A., Lestido-Cardama, A., Vazquez Loureiro, P., Barbosa-Pereira, L., Rodríguez Bernaldo de Quirós, A., & Sendón, R. (2021). Presence of Perfluoroalkyl and Polyfluoroalkyl Substances (PFAS) in Food Contact Materials (FCM) and Its Migration to Food. *Foods*, *10*(7), 1443-. https://doi.org/10.3390/foods10071443

Rampersad, S. N. (2012). Multiple applications of Alamar Blue as an indicator of metabolic function and cellular health in cell viability bioassays. *Sensors*, *12*(9), 12347–12360. https://doi.org/10.3390/s120912347

Richard, A. J., White, U., Elks, C. M., & Stephens, J. M. (2020, April 4). *Adipose Tissue: Physiology to Metabolic Dysfunction* (K. R. Feingold, B. Anawalt, A. Boyce, G. Chrousos, W. W. de Herder, K. Dungan, A. Grossman, J. M. Hershman, J. Hofland, G. Kaltsas, C. Koch, P. Kopp, M. Korbonits, R. McLachlan, J. E. Morley, M. New, J. Purnell, F. Singer, C. A. Stratakis, & D. L. Trence, Eds.). PubMed; MDText.com, Inc. https://www.ncbi.nlm.nih.gov/books/NBK555602/

Roberts, L. D., Murray, A. J., Menassa, D., Ashmore, T., Nicholls, A. W., & Griffin, J. L. (2011). The contrasting roles of PPARδ and PPARγ in regulating the metabolic switch between oxidation and storage of fats in white adipose tissue. *Genome Biology*, *12*(8), R75–R75. https://doi.org/10.1186/gb-2011-12-8-r75

Roberts, S., Hyland, K., Butt, C., Krepich, S., Redman, E., & Borton, C. (2019). *Quantitation of PFASs in water samples using LC-MS/MS large-volume direct injection and solid phase extraction*. https://sciex.com/content/dam/SCIEX/tech-notes/environmental-industrial/water-and-soil/ruo-mkt-02-4707-a/PFAS-Drinking-Water_5500_RUO-MKT-02-4707-A.pdf

Rosato, I., Bonato, T., Fletcher, T., Batzella, E., & Canova, C. (2024). Estimation of per- and polyfluoroalkyl substances (PFAS) half-lives in human studies: a systematic review and meta-analysis. *Environmental Research*, *242*, 117743–117743. https://doi.org/10.1016/j.envres.2023.117743

Rosen, E. D., Hsu, C.-H., Wang, X., Sakai, S., Freeman, M. W., Gonzalez, F. J., & Spiegelman, B. M. (2002). C/EBPα induces adipogenesis through PPARγ: a unified pathway. *Genes & Development*, *16*(1), 22–26. https://doi.org/10.1101/gad.948702

Rotander, A., Toms, L.-M. L., Aylward, L., Kay, M., & Mueller, J. F. (2015). Elevated levels of PFOS and PFHxS in firefighters exposed to aqueous film forming foam (AFFF). *Environment International*, *82*, 28–34. https://doi.org/10.1016/j.envint.2015.05.005

Roth, K., Imran, Z., Liu, W., & Petriello, M. C. (2020). Diet as an Exposure Source and Mediator of Per- and Polyfluoroalkyl Substance (PFAS) Toxicity. *Frontiers in Toxicology*, *2*, 601149–601149. https://doi.org/10.3389/ftox.2020.601149

Ruiz-Ojeda, F. J., Rupérez, A. I., Gomez-Llorente, C., Gil, A., & Aguilera, C. M. (2016). Cell Models and Their Application for Studying Adipogenic Differentiation in Relation to Obesity: A Review. *International Journal of Molecular Sciences*, *17*(7), 1040–1040. https://doi.org/10.3390/ijms17071040

Šabović, I., Cosci, I., De Toni, L., Ferramosca, A., Stornaiuolo, M., Di Nisio, A., Dall'Acqua, S., Garolla, A., & Foresta, C. (2020). Perfluoro-octanoic acid impairs sperm motility through

the alteration of plasma membrane. *Journal of Endocrinological Investigation*, *43*(5), 641–652. https://doi.org/10.1007/s40618-019-01152-0

Saponaro, C., Gaggini, M., Carli, F., & Gastaldelli, A. (2015). The Subtle Balance between Lipolysis and Lipogenesis: A Critical Point in Metabolic Homeostasis. *Nutrients*, *7*(11), 9453–9474. https://doi.org/10.3390/nu7115475

Schrauwen P, Saris WH & Hesselink MK (2001c) An alternative function for human uncoupling protein 3: protection of mitochondria against accumulation of nonesterified fatty acids inside the mitochondrial matrix. FASEB Journal 15, 2497–2502.

Shaikh, O. A., Fatima, A., Shekha, M., Kumar, L., Jaykumar, V., Resham, Ullah, I., & Asghar, M. S. (2023). Forever chemicals: the ugly side of cosmetics. *IJS Global Health*, *6*(4). https://doi.org/10.1097/GH9.0000000000000173

Siersbæk, R., & Mandrup, S. (2011). Transcriptional networks controlling adipocyte differentiation. *Cold Spring Harbor Symposia on Quantitative Biology*, *76*, 247–255. https://doi.org/10.1101/sqb.2011.76.010512

Skurk, T. et al. (2007). Cellular and Molecular A Novel Technique to Propagate Primary Human Preadipocytes without Loss of Differentiation Capacity.

Smith, J., Cianflone, K., Biron, S., Hould, F. S., Lebel, S., Marceau, S., Lescelleur, O., Biertho, L., Simard, S., Kral, J. G., & Marceau, P. (2009). Effects of Maternal Surgical Weight Loss in Mothers on Intergenerational Transmission of Obesity. *The Journal of Clinical Endocrinology and Metabolism*, *94*(11), 4275–4283. https://doi.org/10.1210/jc.2009-0709

Song, J. W., Kim, H. J., Lee, H., Kim, J., & Kwak, Y.-L. (2016). Protective Effect of Peroxisome Proliferator-Activated Receptor α Activation against Cardiac Ischemia-Reperfusion Injury Is Related to Upregulation of Uncoupling Protein-3. *Oxidative Medicine and Cellular Longevity*, *2016*, 3539649–11. https://doi.org/10.1155/2016/3539649

Spangenburg, E. E., Pratt, S. J. P., Wohlers, L. M., & Lovering, R. M. (2011). Use of BODIPY (493/503) to Visualize Intramuscular Lipid Droplets in Skeletal Muscle. *Journal of Biomedicine & Biotechnology*, *2011*, 598358–8. https://doi.org/10.1155/2011/598358

Sukiene, V., Gerecke, A. C., Park, Y.-M., Zennegg, M., Bakker, M. I., Delmaar, C. J. E., Hungerbühler, K., & von Goetz, N. (2016). Tracking SVOCs' Transfer from Products to Indoor Air and Settled Dust with Deuterium-Labeled Substances. *Environmental Science & Technology*, *50*(8), 4296–4303. https://doi.org/10.1021/acs.est.5b05906

Sun, J., Fang, R., Wang, H., Xu, D.-X., Yang, J., Huang, X., Cozzolino, D., Fang, M., & Huang, Y. (2022). A review of environmental metabolism disrupting chemicals and effect biomarkers associating disease risks: Where exposomics meets metabolomics. *Environment International*, *158*, 106941-. https://doi.org/10.1016/j.envint.2021.106941

Sun, W., Zhang, X., Qiao, Y., Griffin, N., Zhang, H., Wang, L., & Liu, H. (2023). Exposure to PFOA and its novel analogs disrupts lipid metabolism in zebrafish. *Ecotoxicology and Environmental Safety*, *259*, 115020–115020. https://doi.org/10.1016/j.ecoenv.2023.115020

Tanaka, T., Yoshida, N., Kishimoto, T., & Akira, S. (1997). Defective adipocyte differentiation in mice lacking the C/EBPβ and/or C/EBPδ gene. *The EMBO Journal*, *16*(24), 7432–7443. https://doi.org/10.1093/emboj/16.24.7432

Tang, Q.-Q., Otto, T. C., & Lane, M. D. (2003). CCAAT/Enhancer-Binding Protein β Is Required for Mitotic Clonal Expansion during Adipogenesis. *Proceedings of the National Academy of Sciences - PNAS*, *100*(3), 850–855. https://doi.org/10.1073/pnas.0337434100

Tarnowski, B. I., Spinale, F. G., & Nicholson, J. H. (1991). DAPI as a Useful Stain for Nuclear Quantitation. *Biotechnic & Histochemistry*, *66*(6), 296–302. https://doi.org/10.3109/10520299109109990

Taub, M., Axelson, E., & Park, J. H. (1998). Colloidal Silica-Coated Tissue Culture Dishes for Primary Cell Cultures: Growth of Rabbit Renal Proximal Tubule Cells. *BioTechniques*, *25*(6), 990–996. https://doi.org/10.2144/98256st01

Teitelbaum, S. L., Mervish, N., L. Moshier, E., Vangeepuram, N., Galvez, M. P., Calafat, A. M., Silva, M. J., L. Brenner, B., & Wolff, M. S. (2012). Associations between phthalate metabolite urinary concentrations and body size measures in New York City children. *Environmental Research*, *112*, 186–193. https://doi.org/10.1016/j.envres.2011.12.006

Trasande, L., Attina, T. M., Sathyanarayana, S., Spanier, A. J., & Blustein, J. (2013). Race/ethnicity-specific associations of urinary phthalates with childhood body mass in a nationally representative sample. *Environmental Health Perspectives*, *121*(4), 501–506. https://doi.org/10.1289/ehp.120552

Tsuyoshi Goto, Joo-Young Lee, Aki Teraminami, Yong-Il Kim, Shizuka Hirai, Taku Uemura, Hiroyasu Inoue, Nobuyuki Takahashi, & Teruo Kawada. (2011). Activation of peroxisome proliferator-activated receptor-alpha stimulates both differentiation and fatty acid oxidation in adipocytes[S]. *Journal of Lipid Research*, *52*(5), 873–884. https://doi.org/10.1194/jlr.m011320

Tunkara-Bah, H., Badjan, H. J., & Senghore, T. (2021). Dietary factors associated with being overweight and obese among school-going adolescents in Region One, The Gambia. *Heliyon*, *7*(3), e06486–e06486. https://doi.org/10.1016/j.heliyon.2021.e06486

VOIGHT, B. F., SCOTT, L. J., MCCULLOCH, L. J., FERREIRA, T., GRALLERT, H., AMIN, N., GUANMING WU, WILLER, C. J., RAYCHAUDHURIL, S., MCCARROLL, S. A., LANGENBERG, C., HOFMANN, O. M., STEINTHORSDOTTIR, V., DUPUIS, J., LU QI, SEGRE, A. V., HOEK, M., NAVARRO, P., ARDLIE, K., … THORLEIFSSON, G.

(2010). Twelve type 2 diabetes susceptibility loci identified through large-scale association analysis. *Nature Genetics*, *42*(7), 579–589. https://doi.org/10.1038/ng.609

Wang, L., Wang, Y., Liang, Y., Li, J., Liu, Y., Zhang, J., Zhang, A., Fu, J., & Jiang, G. (2013). Specific accumulation of lipid droplets in hepatocyte nuclei of PFOA-exposed BALB/c mice. *Scientific Reports*, *3*(1), 2174-. https://doi.org/10.1038/srep02174

Wang, P., Liu, D., Yan, S., Cui, J., Liang, Y., & Ren, S. (2022). Adverse Effects of Perfluorooctane Sulfonate on the Liver and Relevant Mechanisms. *Toxics (Basel)*, *10*(5), 265-. https://doi.org/10.3390/toxics10050265

Wang, Q., Somwar, R., Bilan, P. J., Liu, Z., Jin, J., Woodgett, J. R., & Klip, A. (1999). Protein Kinase B/Akt Participates in GLUT4 Translocation by Insulin in L6 Myoblasts. *Molecular and Cellular Biology*, *19*(6), 4008–4018. https://doi.org/10.1128/mcb.19.6.4008

Wang, S., Cai, Y., Ma, L., Lin, X., Li, Q., Li, Y., & Wang, X. (2022). Perfluoroalkyl substances in water, sediment, and fish from a subtropical river of China: Environmental behaviors and potential risk. *Chemosphere (Oxford)*, *288*(Pt 1), 132513–132513. https://doi.org/10.1016/j.chemosphere.2021.132513

Watkins, A. M., Wood, C. R., Lin, M. T., & Abbott, B. D. (2015). The effects of perfluorinated chemicals on adipocyte differentiation in vitro. *Molecular and Cellular Endocrinology*, *400*, 90–101. https://doi.org/10.1016/j.mce.2014.10.020

Wee, S. Y., & Aris, A. Z. (2023). Environmental impacts, exposure pathways, and health effects of PFOA and PFOS. *Ecotoxicology and Environmental Safety*, *267*, 115663–115663. https://doi.org/10.1016/j.ecoenv.2023.115663

Weppler, A. (2023, March 21). *New Map Shows Location of Known or Suspected PFAS Contamination at Airports and Military Bases across Canada*. Canadian Environmental Law Association. https://cela.ca/blog-new-map-shows-location-pfas-contamination/

Westman, E. C. (2021). Type 2 Diabetes Mellitus: A Pathophysiologic Perspective. *Frontiers in Nutrition (Lausanne)*, *8*, 707371–707371. https://doi.org/10.3389/fnut.2021.707371

White, U. A., Fitch, M. D., Beyl, R. A., Hellerstein, M. K., & Ravussin, E. (2017). Association of In Vivo Adipose Tissue Cellular Kinetics With Markers of Metabolic Health in Humans. *The Journal of Clinical Endocrinology and Metabolism*, *102*(7), 2171–2178. https://doi.org/10.1210/jc.2016-4000

Wilcox G. (2005). Insulin and insulin resistance. *The Clinical biochemist. Reviews*, *26*(2), 19–39.

World Health Organization. (2024, March 1). *Obesity and overweight*. World Health Organization. https://www.who.int/news-room/fact-sheets/detail/obesity-and-overweight

Wu, Z., Rosen, E. D., Brun, R., Hauser, S., Adelmant, G., Troy, A. E., McKeon, C., Darlington, G. J., & Spiegelman, B. M. (1999). Cross-Regulation of C/EBPα and PPARγ Controls

the Transcriptional Pathway of Adipogenesis and Insulin Sensitivity. *Molecular Cell*, *3*(2), 151–158. https://doi.org/10.1016/S1097-2765(00)80306-8

Yamamoto, J., Yamane, T., Oishi, Y., & Kobayashi-Hattori, K. (2015). Perfluorooctanoic acid binds to peroxisome proliferator-activated receptor γ and promotes adipocyte differentiation in 3T3-L1 adipocytes. *Bioscience, Biotechnology, and Biochemistry*, *79*(4), 636–639. https://doi.org/10.1080/09168451.2014.991683

Yang, J., Fan, S., Zhang, Y., Huang, M., Gao, Y., & Bi, H. (2022). Chronic Treatment With WY-14643 Induces Tumorigenesis and Triglyceride Accumulation in Mouse Livers. *Drug Metabolism and Disposition*, *50*(12), 1464–1471. https://doi.org/10.1124/dmd.122.000908

Yao, Z., Gong, Y., Chen, W., Shao, S., Song, Y., Guo, H., Li, Q., Liu, S., Wang, X., Zhang, Z., Wang, Q., Xu, Y., Wu, Y., Wan, Q., Zhao, X., Xuan, Q., Wang, D., Lin, X., Xu, J., Zhao, J. (2023). Upregulation of WDR6 drives hepatic de novo lipogenesis in insulin resistance in mice. *Nature Metabolism*, *5*(10), 1706–1725. https://doi.org/10.1038/s42255-023-00896-7

Yook, J.-S., You, M., Kim, Y., Zhou, M., Liu, Z., Kim, Y.-C., Lee, J., & Chung, S. (2021). The thermogenic characteristics of adipocytes are dependent on the regulation of iron homeostasis. *The Journal of Biological Chemistry*, *296*, 100452–100452. https://doi.org/10.1016/j.jbc.2021.100452